Three-dimensional display technologies of recent interests – principles, status and issues[◊]

Jisoo Hong,[1] Youngmin Kim,[1] Heejin Choi,[2] Joonku Hahn,[3] Jae-Hyeung Park,[4] Hwi Kim,[5] Sung-Wook Min,[6] Ni Chen,[1] and Byoungho Lee[1,*]

[1]School of Electrical Engineering, Seoul National University, Gwanak-Gu Gwanakro 599, Seoul 151-744, Korea

[2]Department of Physics, Sejong University, 98 Gunja-Dong, Gwangjin-Gu, Seoul 143-747, Korea

[3]School of Electronics Engineering, Kyungpook National University, 1370 Sankyuk-dong, Buk-gu, Daegu 702-701, Korea

[4]School of Electrical & Computer Engineering, Chungbuk National University, Heungduk-Gu, Cheongju-Si, Chungbuk 361-763, Korea

[5]Department of Electronics and Information Engineering, College of Science and Technology, Sejong Campus, Korea University, Jochiwon-eup, Yeongi-gun, Chungnam 339-700, Korea

[6]Department of Information Display, Kyung Hee University, Dongdaemoon-ku, Seoul 130-701, Korea

[*]Corresponding author: byoungho@snu.ac.kr

Recent trend of three-dimensional (3D) display technologies is very interesting in that both old-fashioned and up-to-date technologies are actively investigated together. Release of the first commercially successful product of 3D display raised new research topics in stereoscopic display. Autostereoscopic display renders a ray field of 3D image whereas holography replicates

a wave field of it. Many investigations are conducted on those next candidates of commercial product to resolve existing limitations. Up-to-date see-through 3D display is a concept close to an ultimate goal to presenting seamless virtual images. Though it is still far from practical use, many efforts are made to resolve issues like occlusion problem.

OCIS codes (110.2990) Image formation theory, (100.6890) Three-dimensional image processing

◊Data sets associated with this article are available at http://midas.osa.org/midaspre/item/view/1012?key=a3d6VGVGRlUzZEZKdw==. **Links such as "View 1" that appear in figure captions and elsewhere will launch custom data views if ISP software is present.**

1. Introduction

Three-dimensional (3D) display has a long history starting from the first suggestion of a stereoscope by Wheatstone in the mid-19th century [1] through active inventions of various autostereoscopic technologies in the late 19th and early 20th centuries, an era of holography in the 1960's and 1970's and adoption of digital devices today. Though most of basic ideas have been proposed more than tens of years ago or even hundred years ago, none of them are without critical issues that are obstacles to catch a mass market. Since late 1990's, a development in digital devices led to a widespread of flat panel display (FPD) especially based on the liquid crystal (LC) technology. It was a catalyst to the research on implementing commercially acceptable 3D display again. From Fig. 1, the recent research trend on 3D display can be inferred. It is interesting to see that research on autostereoscopic displays including parallax barrier, integral imaging (InIm) and lenticular lens has grown continuously starting from the year around 2000 when the LC display (LCD) became popular. Especially, parallax barrier, which is more suitable for implementation with LCD, shows steeper increase compared with other autostereoscopic technologies. Despite increasing research interest and demand from market, up to a few years ago, it was a major opinion that 3D display was still far from mass commercialization.

Recent few years will be marked as "historic" in the history of 3D display because, for the first time, several major manufacturers in the display industry started to supply successful commercial products based on the stereoscopy to the massive market. Stereoscopy is a technology that has history of more than 170 years and there have been no notable breakthrough

other than researches and inventions conducted in its early decades. The only difference in the circumstance is that a value chain of the industry started to work with 3D films, which became common and popular in ordinary theaters after the success of a monumental movie 'Avatar'. Commercialization revealed new issues of stereoscopy in the aspects of product and 3D became again a very active research topic now. Nowadays the research trend in the field of 3D display is very interesting: old-fashioned technologies such as stereoscopy and science fiction movie-like fancy technologies are actively and popular together as research topics. This phenomenon comes from a larger time lag of commercialization to latest technologies compared with other industries. In this tutorial paper, recent research interests of 3D display will be outlined covering both product-focused and up-to-date technologies.

2. Depth cues in perceiving 3D images

Human visual system (HVS) perceives 3D information of an input image by various depth (or distance) cues which can be categorized as psychological and physiological cues. Psychological cues are associated with a process inside a brain to analyze visual information based on the trained experiences. HVS can infer rough 3D information from even two-dimensional (2D) images such as ordinary photographs with psychological cues if it does not include artificial contradictions or ambiguous relationships. In contrast, physiological cues are information related to a physical reaction of human body when 3D image is given to HVS. Physiological cues can provide more exact 3D information without ambiguity. The objective of 3D display is to reproduce 3D image by using various depth cues to stimulate HVS.

Psychological cues include linear perspective, overlapping, shading and texture gradient, and so on. These representative psychological cues are described in Fig. 2(a) and they are trained through everyday life. Of course, they are not all of the psychological cues but countless

empirical data is also used to analyze an image. However such an image-based approach always involves ambiguities and errors because it could not provide complete real depth information. With only psychological cues, it is understanding of 3D information rather than feeling it. Because of such ambiguities and errors, investigations on extracting depth information from single 2D image based on psychological cues do not show satisfactory results yet. If a display system is to be categorized as 3D display, it should provide not only psychological but physiological depth cues.

Figure 2(b) briefly describes reactions of human body related to a series of physiological depth cues. Binocular disparity or stereopsis, which is most prominent among physiological depth cues, is acquiring depth information from parallax appearing in two images obtained from left and right eyes. Because it gives most part of 3D information that can be obtained from physiological cues, early 3D displays based on a binocular disparity. Stereoscopic or autostereoscopic displays are categories that use only binocular disparity among physiological depth cues. Actually, the term "autostereoscopic display" itself only means that it can give stereopsis without any special apparatus hence it does not imply a restriction to other physiological cues. However it is usual to classify 3D displays with other physiological cues as volumetric display. Though stereoscopic or autostereoscopic displays provide sufficient 3D information to observers, visual fatigue or discomfort was always a challenging issue of using them as a commercial 3D display. It is still unclear what really causes it however researchers believe that conflicts between information obtained from artificially produced cues may be a reason. There are other physiological cues such as ocular convergence and accommodation as shown in Fig. 2(b). Ocular convergence is a reaction to rotate ocular globes to create a fixation point at a location of 3D object in interest. Accommodation is to control an eye lens to make

clear image of 3D object on retina. In stereoscopic or autostereoscopic displays, convergence is usually satisfied while accommodation is always not because the images are in focus on the display. It is believed that such conflict can be a reason of visual fatigue [2]. Other than such accommodation-convergence mismatch, error in vertical disparity and crosstalk between left and right images can disturb stereoscopic relationship and they can be other reasons to visual fatigue [3]. Many investigations are conducted to reduce or eliminate such issues in stereoscopic or autostereoscopic displays however there is no definite way yet. Volumetric display such as holography is an approach to resolve such issues by providing all of physiological depth cues. Though it is a definite way to deal with visual fatigue, it requires huge amount of information in implementation. Hence it is more future technique in a roadmap of 3D display.

3. Stereoscopic 3D display technologies

Stereoscopic 3D display technologies use special glasses to induce binocular disparity and convergence by providing different left-eye and right-eye images to the observer. Generally, they are categorized according to the types of the glasses – LC shutter glasses and polarization glasses. Recently, with the improvements of FPD technologies, the stereoscopic 3D display could reach the level of commercialization and several stereoscopic 3D products are on sale in the market. One of the most advantageous features of those stereoscopic 3D products is that they can be made using the existing FPD manufacturing processes and therefore require a little additional cost. As a result, the stereoscopic 3D products are regarded as an important step in the advance for the popularization of 3D display technologies. By now, there are three stereoscopic 3D display technologies adopted or to be adopted in the 3D monitors and TVs. Among them, one requires LC shutter glasses while the others need polarization glasses and polarization modulators for the additional 3D devices. In this section, the basic principles and structures of

the above three technologies will be reviewed and their pros and cons will also be compared. Although the stereoscopic 3D display can be realized using an LCD, a plasma display panel (PDP), or an organic light emitting diode (OLED) display, the review in this section is based on the case of stereoscopic 3D LCD since most of the stereoscopic 3D products use LCD panels as display devices.

The first one to review is a 3D technology with LC shutter glasses. The LC shutter glasses are composed of two active LC shutters which can open and block the observer's left-eye and right-eye separately. With the operation of LC shutters, the glasses can make the observer watch images displayed on the display panel only through the left-eye or right-eye. As a result, if the display panel shows the left-eye and the right-eye images in different frames in a synchronized manner with the operation of LC shutter glasses, the observer may feel the binocular disparity and convergence from the recognized images. For realizing a stereoscopic 3D display with the above principle, a display device with frame-rate higher than 120 Hz or 240 Hz, a wireless protocol for connection and synchronization of LC shutter glasses with display device, and a technology for fast LC shutter are required. These devices are already commercialized. Therefore, it is possible to realize a 3D display with LC shutter glasses with minimum additional cost. However, there are some factors to be regarded in arranging the left-eye and the right-eye images in different image frames. In case of using an LCD panel as a display device, the left-eye and the right-eye images are switched in a sequence of line by line (progressive scan). Hence it is needed to add a separation frame between the left-eye and the right-eye image frames. As an image of separation frame, a black image is commonly used and an additional backlight operation such as scanning or blinking can be added to enhance the quality of 3D images. Figure 3 shows the principle of stereoscopic 3D display with LC shutter glasses using 240 Hz LCD

panel with a sequence of Left-eye image frame → Black frame→ Right-eye image frame → Black frame (LBRB) operation and an additional backlight operation [4, 5].

Since the left-eye and the right-eye images are displayed in different frames using all pixels in the display device, the 3D technology using the LC shutter glasses has no resolution degradation in displaying 3D images. In other words, current 3D monitors or TVs using LC shutter glasses can realize a Full-HD (1920 x 1080 pixels) 2D and 3D images. Since the resolution is one of the key factors of image quality, the 3D technology using LC shutter glasses has an advantage in this aspect. Moreover, the LBRB operation can be adopted by a minor revision of image processing unit in the 2D LCD module. As a result, the 3D technology with LC shutter glasses requires a minimum level of change in the structure of 2D LCD module and becomes a most practical solution for 3D products. However, the technology also has some issues to be improved. At first, due to the inserted black image frames and shuttering operations in glasses, the luminance of the 3D image reduces to lower than quarter of that of 2D image. Secondly, in case of slow LC response, a residual image of the black image (no image) frame can remain and become a cause of 3D crosstalk, i.e., the overlapping of the left-eye and the right-eye images. The backlight operation such as scanning or blinking is to prevent the 3D crosstalk by compensating the incomplete response of LC. The last one is that the weight and the price of LC shutter glasses are higher than those of polarization glasses due to the adoption of electronic devices. Therefore, researchers are trying to make progresses on the above issues and recently a 3D TV with LC shutter glasses and 240 Hz UD (3840x2160) LCD panel has been exhibited in Display Week 2011 by Samsung Electronics.

The next two stereoscopic 3D display technologies use polarization glasses to induce the binocular disparity and convergence. The basic principle of those methods is to adopt a

polarization modulator in the display device to make the left-eye and the right-eye images have orthogonal polarization to each other. Therefore, the polarization glasses are composed of two polarization filters to separate the left-eye and the right-eye images with orthogonal polarizations. In modulating the polarization of the left-eye and the right-eye images, there are two different methods – spatial modulation and frame modulation. The former one is called a patterned retarder (PR) while the other is known as active retarder (AR) or shutter in panel (SIP). The principle of PR method is to display an interleaved mixture of the left-eye and the right-eye images and to impose the polarization of them using a PR. Since the LCD panel itself has a linear polarizer on its top (front) surface, it is possible to make the left-eye and the right-eye images have left-handed and right-handed circular polarizations by inducing phase retardations with π-difference. Since it is common to arrange the left-eye and the-right eye images to have only odd or even pixel lines (line-by-line arrangement) the PR needs to have same structure and to be aligned with high accuracy to prevent the 3D crosstalk. Figure 4 shows the structure and principle of the PR technology [6].

In the example of Fig. 4, the LCD panel is assumed to have 8 pixel lines and the left-eye and the right-eye images have 4 pixel lines each. However, for current 3D TV with PR technology, an LCD panel with a Full-HD resolution is commonly used and the number of pixel lines for each eye's images is 540. The PR method does not need to insert the black image frame and the luminance of 3D image is almost two times higher than that of the 3D technology with LC shutter glasses. Moreover, the slow response of LC does not affect the 3D crosstalk since the left-eye and the right-eye images are displayed in a single frame. The use of lighter and cheaper polarization glasses is another attractive point and the use of circular polarization to separate the images allows the observers to rotate their head without a concern of luminance degradation. In

spite of those advantages, the early models of PR technology used a glass PR filter with a high manufacturing cost and resulted in only a small volume of sales. In this year, with a new technology (by LG Display) to replace the glass PR with a film PR (FPR), the manufacturing cost of FPR 3D TVs was considerably reduced and the price of them is lower than the 3D TV with LC shutter glasses, while the above advantages are conserved.

The 3D resolution of FPR method is still under discussion. Although it is clear that the left-eye and the right-eye images have half numbers of pixel lines, there are two opinions in opposite positions. The first one is that the 3D resolution of FPR 3D TV is same as that of the left-eye and the right-eye images and is only half of 2D resolution. In other words, an FPR 3D TV with Full-HD LCD panel has a half Full-HD 3D resolution with 540 pixel lines. The manufacturer of 3D display with LC shutter glasses is supporting this opinion. In contrast, the manufacturer of FPR 3D display is claiming that the 3D image recognition is done by a combination of the left-eye and the right-eye images and therefore has a Full-HD resolution with 1080 pixel lines. A demonstration has been proposed by the FPR manufacturer to count the number of lines with moving the 3D image by one line each time and the result was that 1080 movements were counted. Several organizations such as Interteck and the 3rd Institute in China and Verband Deutscher Elektrotrchniker (VDE) in Germany have verified the above demonstration, while another organization, Consumer Reports in USA, is in a negative side about it even though they listed the FPR 3D TV at No. 1 position in performance test among the 3D TVs sold in USA.

The last stereoscopic 3D display technology which is called AR or SIP requires passive polarization glasses but a time-sequential polarization modulator. The basic principle of AR or SIP technology is to display the left-eye and the right-eye images in different frames with

orthogonal polarizations and those images are seperated by polarization glasses [7]. For that purpose, the time-sequential polarization modulator needs to operate with speed faster than 120 Hz and the display device has to be synchronized with it as shown in Fig. 5.

With the structures and principles above, it can be thought that the polarization glasses and the AR have the same role as the LC shutter glasses. Therefore, the 3D TV using AR technology can provide a Full-HD 3D image with almost the same luminance as that of FPR method. However, similar to the case of LC shutter glasses, a special technique such as black image frame insertion may be required to synchronize the operation of AR with the switching of the left-eye and the right-eye images because of the progressive scan, and the luminance of 3D image may be reduced. Another weak point of the AR technology is that the manufacturing cost of AR or SIP itself is expected to be higher than others. Since the AR or SIP is also an active LCD panel with simpler structure, the 3D display with AR method is actually composed of two LCD panels. Considering that the LCD panel is the most expensive part of an LCD module, it is not easy for the 3D display with AR technology to achieve a competitive price. However, there are continuous researches on the AR or SIP technology for the next generation stereoscopic 3D products and recently 3D notebook PC, 3D monitor, and 3D TV based on the SIP technique are exhibited in Display Week 2011 (May 2011, Los Angeles, CA).

Although each of the above stereoscopic 3D display technologies has its own pros and cons, there are a common advantage and a common issue to be improved for all of them. As described above, the most advantageous point is that the stereoscopic 3D products can show 3D image with high quality and low cost. However, the need of wearing 3D glasses is a major concern no matter what kind of the glasses are. The NPD Group in USA has announced that the 42 percent of consumers who will not buy the 3D TV answered that the 3D glasses were not

comfortable to them. Therefore, researchers in 3D technology are trying to realize a practical autostereoscopic (without using glasses) 3D display. The details of autostereoscopic 3D technology will be reviewed in the following sections.

4. Autostereoscopic 3D display technologies

4.1. Lenticular lens

The lenticular lens technology is to attach a one-dimensional array of lenticular lenses to distribute the pixels of display device to multiple viewpoints. The role of lenticular lens is to magnify and transfer the information of specific pixels to a designated position as shown in Fig. 6. Therefore, the observers in different viewpoints can watch different images and binocular disparity, convergence, and motion parallax can be realized. However, since it is impossible for the observer to watch all pixels at once, the 3D resolution is reduced and there is a trade-off relation between the resolution of 3D image and the number of viewpoints. In spite of the above weak point, the lenticular lens technique is expected to be suitable for the early outdoor 3D digital signage because it can provide 3D images with high luminance.

Since it is obvious that the resolution of 3D image should be reduced in lenticular lens system, there are two advanced techniques to compensate it. One of them is a slanted lenticular system to distribute the loss of resolution into both horizontal and vertical directions by slanting the structure of lenticular lens or rearranging the color filter of pixels [8]. The other is the LC lens technology which enables the lenticular lens display system to become a switchable 2D/3D display by generating or eliminating the lenticular lens electrically. In the early age, a refractive LC lens was commonly used for the above role. However, due to the problems which come from the thickness of the refractive LC lens, the researchers are trying to develope a practical

diffractive LC lens nowdays [9-12]. Figure 7 shows operations of 2D/3D lenticular lens using patterned electrode method developed by LG Electronics recently. The electric field at the part of lens edge is much stronger than electric field at center of lens. This non-uniform distribution of electric field causes non-uniform distribution of tilt angle of LC director and the refractive index distribution changes accordingly.

4.2. Parallax barrier

Parallax barrier is much similar to the lenticular lens in fundamental principle showing 3D images. Instead of using lenticular lens sheet, parallax barrier adopts an array of vertical masks to show different views to left and right eyes. As shown in Fig. 8(a), if an array of vertical masks (or slits) was properly designed, there will be a certain viewing position where each eye can see only even or odd columns of pixels through slits between masks. Hence the left and right eyes watch different images composed by only even or odd columns of pixels and it stimulates stereopsis. Parallax barrier setup can be easily extended to a multi-view case by expanding a size of each mask. Roughly an array of vertical mask whose mask pitch is *n* times larger than pixel pitch of display panel gives *n* views. Parallax barrier has the same resolution reduction problem as a lenticular lens display because it also uses pixel multiplexing to impose left and right images. More severe problem is a reduction of brightness of images because it blocks light from pixels with masks to implement an autostereoscopic feature. And it becomes worse for a multi-view case because a total area of mask is increased. Despite those disadvantages, parallax barrier is popular autostereoscopic technology among manufacturers because it can be easily implemented without an additional optic element and give 2D/3D convertible feature by using LC panel as vertical masks. By simply displaying an image of array of vertical masks on additional LC panel, 3D display mode is utilized. 2D display mode can be achieved by displaying a white image on an

additional LC panel. LC panel becomes just a transparent glass and the 2D image on a display panel behind is directly shown to an observer as shown in Fig. 8(b). Another advantage of adopting LC panel as an array of vertical masks is that it can be used to resolve a reduction of resolution. Basically a reduction of resolution comes from the situation where information of image is given only through the location of each slit. By continuously shifting an array of vertical masks with a step size of slit pitch, a full resolution of display panel can be perceived by an observer. Though it requires higher frame rate for display panels incorporated in a system to provide a natural afterimage without flickering, a series of investigations are conducted to resolve a reduction of resolution by using this scheme [13,14].

Sharp already tried to distribute commercial cellphones adopting a parallax barrier through a vendor NTT DoCoMo in Japan, 2002. However the result was not successful because of a lack of compatible contents. The second trial was made by Samsung Electronics in Korea, 2007. A cellphone with parallax barrier feature was released by Samsung Electronics and it even had a stereo-camera to overcome a lack of contents. However the 3D display feature was not emphasized at all for marketing and it left no impressive mark in the history of 3D display. On June 2011, LG Electronics released a smartphone with parallax barrier and stereo-camera globally and 3D display feature is a main marketing point for this product. Many people believe that this third trial of commercial autostereoscopic product will be successful because of positive mood in 3D display industry and increasing number of compatible contents.

4.3. Integral imaging

Integral imaging, originally called integral photography, is a promising 3D display technique with more than 100 years of history [15]. It was the first proposal among autostereoscopic displays, such as lenticular lens method, parallax barrier method, integral

imaging, and even holography. Integral imaging uses an array of small lenses that are spherical, square or hexagonal to produce the 3D images which can provide both horizontal and vertical parallax, resulting from a 2D lens array. Unfortunately, the reason why integral imaging did not prosper in early days was that lens arrays were not economically feasible for practical use until World War II. Before then, a pinhole array, which is optically equivalent to the lens array, had been used for the most of integral imaging researches. However, the 3D image with low brightness, which results from the small pinhole aperture size, was not proper for a commercial use. Another reason that integral imaging was not attractive in the early years of invention was a recording device. The first integral imaging was 'integral photography,' which was to record a complete spatial image on a photographic plate with horizontal parallax as well as vertical parallax. The method was a huge breakthrough for 3D display; however, all the methods of using photographic plate for recording and displaying an image were not suitable for moving objects. The bottleneck was overcome by mass production of micro lens array and development of active recording and displaying devices, such as high-resolution digital cameras and two-dimensional flat panel display device. Hence the technologies enabled integral imaging to evolve as the real-time process system [16].

The structure and concept of the integral imaging system are illustrated in Fig. 9. In pickup step, each individual lens or pinhole will record its own micro image of object, which is called elemental image and a large number of small and juxtaposed elemental images will be produced behind the lens array onto the recording device. In display step, the display device with elemental image is aligned with the lens array and a spatial reconstruction of the object is created in front of the lens array, which can be observed with arbitrary perspective within a limited viewing angle. Therefore, integral imaging suffers from inherent drawbacks in terms of viewing

parameters, such as viewing angle, resolution, and depth range due to limited resolution of the 2D FPD and lens array itself [17].

In spite of recent many advanced researches of integral imaging, most of them can be categorized into two methods, real/virtual display mode and focused display mode [18-20]. The difference of each mode, as shown in Fig 10, is the gap between 2D lens array and elemental image on the display device. In the focused display mode, the gap between 2D lens array and elemental image is equal to the focal length of the lens array. This was the original integral photography proposed in 1908 [15]. In this mode, the rays from each elemental image pixel are collimated by the corresponding elemental lens in ideal case, so the resolution of the recreated 3D image is deteriorated, resulting from magnification of elemental lens. In regards of depth range of the focused display mode, in theory, it provides wide range of depth because the beam waist from each ray bundle is minimized at the lens array and it increases as the beam propagates. In this focused display mode, both real and virtual images can be integrated with about the same resolution. On the contrary, in real/virtual display mode, the gap is set to be larger or smaller than the focal length of the lens array. Therefore the image distance with good focus of image of each ray bundle from elemental image pixel is determined by the focal length of the lens array and the gap between the 2D lens array and the display device in accordance with the Gauss lens law. The recreated 3D image is formed around the image plane of the 2D lens array. Here the image plane is called the central depth plane (CDP). As the reconstructed point of the 3D image goes away from the CDP, beam waist from each ray bundle increases, which results in degradation of recreated 3D image. In other words, the real/virtual display mode is better in image quality of reconstructed 3D image around the CDP and the depth range of 3D image is limited around the CDP.

The limitation of viewing angle occurs when the elemental images are observed not through corresponding elemental lenses but through neighboring lenses. Each elemental lens has its corresponding area in the elemental image plane, and the elemental images should be placed inside the corresponding area in order to prevent cracking or flipping of reconstructed 3D image. The viewing angle is determined by the pitch of lens array and the gap between lens array and display device. The individual ray bundle from elemental image pixel can be distributed by lens array, so the number of perspectives within viewing angle is understood as angular resolution. If other conditions such as the pitch of elemental lens and the gap between lens array and display device are equal as the resolution of display device increases, then, integral imaging can provide more natural views because of high angular resolution density [21]. Super multi-view condition can be achieved when angular resolution density of individual ray bundle is high enough for providing number of views into the single eye [22].

The distinctive feature of integral imaging compared to the lenticular lens method or parallax barrier method is to use 2D lens array. The 2D lens array structure enables both horizontal parallax and vertical parallax to be provided. However, the main trade-off for the full parallax is lower resolution of the reconstructed 3D image compared with previously mentioned autostereoscopic display techniques, such as lenticular lens method or parallax barrier method. This is the main reason why researchers in industry prefer one-way parallax, mostly horizontal-parallax-only (HPO) method, rather than integral imaging. However, as the resolution of 2D flat panel display increases, the resolution of 3D image based on integral imaging is expected to be higher in near future. Therefore integral imaging can be an alternative, lying between stereoscopic display and holography. Another issue with regard of 2D lens array is the color moiré pattern, which can degrade the image quality of integral imaging [23, 24]. The color moiré

pattern usually comes from the periodicity of overlapped similar structures of color pixel and 2D lens array. Typically the 2D flat panel device that provides elemental images expresses arbitrary color images by the combination of red (R), green (G), and blue (B) pixels. Although each pixel has individual arrangement and different sizes, they have periodicity. Because of similar periodicity of 2D lens array, the former interferes with the periodicity of 2D lens array. In such a case, a visible color periodic pattern (usually vertical lines) will be generated (In general, projection-type integral imaging is free from color moiré pattern problem.) [25]. To resolve the moiré pattern in integral imaging, some methods have been proposed as the alternatives. The simplest method is to break the periodicity of overlapped structures - a color pixel array or lens array. The former can be implemented by changing the layout of the color filter on flat panel display device [23], and the latter can be effective when slanted lens array is placed in juxtaposition with display device [24]. Because change of the layout of the color filter is hampered by a variety of restrictions, the slanted lens array method is a viable alternative to the color moiré pattern problem. Figure 11 shows the simulation results according to the rotated angle of the lens array on the display panel.

Since the viewing parameters discussed above have trade-off relationship, the simultaneous enhancement of them is possible by manipulating each component of integral imaging. Some theoretical studies on these issues have been reported by using ray optic analysis as well as wave optic analysis [18, 26, 27]. Theoretical analysis for integral imaging performance was also quantitatively done [28]. In the following, we shall focus on reviewing recent researches to mitigate those issues. Display hardware system for enhancement of viewing parameters in integral imaging will be presented mainly.

One of the challenging problems in integral imaging is extending the viewing angle. Once the pitch of elemental lens and the gap between lens array and display device are set, the viewing angle is also determined. The viewing angle enhancement can be accomplished by enlarging the area in the elemental image that corresponds to each elemental lens or altering the structure of lens array. One of the best ways to deploy the elemental image area is using mechanical dynamic movement of lens array or barrier [29-32]. Moving the lens array in synchrony with a high speed update of the pixel content can increase the viewing angle [29]. Another approach for enhancing viewing angle without mechanical movement of optical components is to double the region of each elemental image by using orthogonal polarization switching [33]. Another recent approach to improve viewing angle of integral imaging is to apply adaptive elemental image by using head tracking system, which is effective only for a small number of users [34], as shown in Fig. 12(a). The methods to modify configuration of lens array or display device are noticeable [35-40]. A horizontal viewing angle of 66° for 3D images was achieved experimentally using curved lens array and screen as shown in Fig. 12(b) [37], and 360°-viewable integral imaging system using flexible backlight was implemented [38]. Instead of changing total structure of lens array or screen, embossed screen for projection-type integral imaging was proposed [39]. The use of multiple axis telecentric relay system which allows the substantial increase of the field of view (FOV) of any micro lens provides the elemental images with proper directions, increasing the viewing angle of integral imaging [41]. A theoretically investigated research was reported by using a negative refractive index planoconcave lens array and inserting high refractive index medium between elemental image and lens array [42, 43]. Recently, enhancing the uniformity of the angular resolution within viewing angle by using boundary folding mirrors has been studied [21].

Resolution enhancement is mainly achieved by increasing the bandwidth of the information on the display device, which can be done by reducing pixel size of display device and using a temporal or spatial multiplexing scheme [44-47]. Recently, with the rise of development of 2D FPD device, a high definition display device is used for providing enhanced 3D image resolution. However, electrically or mechanically moving lens array (pinhole array) method or rotating prism sheet method can be an alternative for better viewing resolution because there is a physical limit to the reduction of pixel size of display device [28, 29, 44, 45]. Spatial multiplexing method is mainly performed by tiling display devices for the entire elemental image as shown in Fig. 13 [46, 47]. In this case, alignment among elemental images and lens array arrangement is another important issue.

Although integral imaging can provide depth range to some extent, the simplest way for depth range enhancement is to create multiple image planes (or CDPs) of elemental images by combining plural display devices because the depth range is formed around the CDP. Figure 14 shows some examples of the configuration for enhancing image depth range. The depth range enhancement can be realized by mechanically moving the elemental image plane, stacking display devices, such as LCD or polymer dispersed liquid crystal (PDLC), and using a birefringent plate [48-55]. Another approach for depth range enhancement is to combine floating displays with the integral imaging [56-62]. By using a large convex lens or a concave mirror to display the image of an object to observer, the floating display method can provide an impressive feel of depth. Although the image source of integral floating display is provided by the integral imaging method, the reconstructed image produced by integral floating display has different viewing characteristics compared with the reconstructed 3D image by integral imaging method.

2D/3D convertible display is an important issue for the penetration of 3D display market because it can be a stepping stone between 2D and 3D display. In integral imaging, various types of 2D/3D convertible display have been proposed as well. The key issue of 2D/3D convertible integral imaging method is controlling activation of the lens array or pinhole array. In one approach, the activation can be achieved by electrically controllable diffuser made of PDLC or transparent LCD panels [63, 64]. Finally, for controlling point light source array, various methods have been reported by using pinholes on a polarizer, light emitting diode (LED) array, plastic optical fiber array, an OLED panel, or a punctuated electroluminescent film [65-70].

Recent progress of autostereoscopic displays is focused on the enhancement of 3D resolution as well as smooth parallax. Although integral imaging provides both vertical and horizontal parallax within limited viewing angle, low resolution resulting from full parallax is still a problem for practical use. Recently 21 inch 3D LCD TV with high definition (1280 × 800) was revealed, which is one of the most qualified integral imaging systems using 2D FPD. However, it is not practical yet because of the need of ultra-high definition (UHD) panel, the manipulation of micro lens array, and alignment issue between lens array and display device. For example, for achieving the resolution of 200 × 200 and the ray density per single elemental lens of 5 × 5, we need an XGA panel (1024 × 768) at the least. When it expands to the smooth parallax for natural views, UHD panel will be necessary for the same 3D resolution of reconstructed image. Currently available FPD, on the contrary, provides full HD resolution (1920 × 1080) and 120 or 240 Hz refresh rate. The resolution of 3D image is expected as the resolution of full HD or equivalent. However, the resolution remains as XGA resolution in practice even though UHD panel and fine micro lens array are used. Therefore, to process the high-density information of integral imaging in real-time, more than UHD display device, fast

LC response time with high speed driving circuit and micro lens manufacturing technology are necessary for mass production. As in the lenticular lens system, electrically controllable 2D LC lens array is a good research direction.

5. Holography

Holography was invented by Gabor as a new concept of electron microscopy [71]. This technique presents a feasibility in reconstructing signal waves with magnification. Then, holography has received lots of interests after the development of laser technology. Leith and Upatnieks proposed off-axis holography to separate a signal from its autocorrelation and conjugate with carrier frequency [72]. Various media for recording had been applied and developed in the same period. Volume hologram was invented by Denisyuk and it records interference on thick reflection hologram [73]. This invention was regarded as a work originated from a color photography plate by Lippmann [74].

The first digital hologram was computed and implemented by Lohmann and Paris [75] and the principle on digital holography was straightened out by Goodman and Lawrence [76]. Digital holography technology has powerful potential to record an optical wave and reconstruct it dynamically using electro-optical devices. Originally the digital holography meant reconstruction of hologram using computer. But, recently this terminology is widely used for representing holography using electronic devices or computers in either recording or reconstruction. Even though there are notable improvements for recording technique [77-79], it is regarded as impractical to capture an interference between reference wave and signal wave reflected from real dynamic objects. As computational power increases, computer-generated holography is expected to be a promising technology to provide contents for digital holographic display.

5.1. Principle

Digital holography is realized with electro-optical devices for recording and reconstruction. Since most electro-optical devices have a rectangular sampling lattice, the signal measured or retrieved by them fundamentally follows the Whittaker-Shannon sampling theorem. Even though any band-limited function cannot be perfectly space-limited, it is possible to represent a band-limited function with a finite number of samples with practical accuracy. The product of the area of sampled space and its bandwidth is referred to as the space-bandwidth product (SBP). When the optical signal is reconstructed by digital holographic method, the SBP of this wave has a finite number and its value is equal to the number of sampling points in the electro-optical device retrieving the wave [80]. That is, if the number of sampling points is fixed in an optical system, the SBP is also determined as the same number. For example, spatial light modulators (SLMs) have a finite number of pixels and this number means its SBP. For a given SLM, it is impossible to increase the size of reconstruction image without the cost of its bandwidth.

In holography an SLM is mostly applied as amplitude-only or phase-only modulation device for reconstructing a desired wave, even though the technique for realizing complex modulations has been studied and implemented. As Oppenheim and Lim pointed out [81], the phase in signals has more important meaning than its amplitude information especially in Fourier transform. In practice, there is a benefit to design a display system with Fourier transform since the autocorrelation of collimated reference is focused on a point and it may be easily filtered out. In Fourier transform, a view volume reconstructed by an SLM is bounded as a wedge shape as shown in Fig. 15 when we consider the overlap among higher-order diffraction terms [82]. The signal bandwidth free of aliasing is identified as Nyquist frequency and there is its replica array

arranged in rectangular lattice. Hence higher order terms determine a view volume in 3D space and inside it diffracted wave is displayed without conflicts by its replica.

The displayed view volume has transverse and longitudinal resolutions since the SBP is finite. The resolution of the view volume is determined by the Fourier uncertainty relationship, meaning that the resolution is inversely proportional to the bandpass [83]. Since angular spectrum is a Fourier transform of the signal, the bandwidth at SBP can be understood as the bandwidth of angular spectrum. Therefore, the resolutions are given by $\lambda z_0 / A$ in the transverse coordinates and $8\lambda z_0^2 / A^2$ in the longitudinal coordinate, where λ is the wavelength used for a digital holographic display system and z_0 is the distance from Fourier transform lens to the interested position in a view volume. The aperture size A is regarded as the width of SLM that is equal to the width of sampled area.

In a similar sense, the quality of reconstructed wave is delicately evaluated as a quality metric [84]. In general we assume that a point is reconstructed by an SLM without an additional optic devices or lenses. In this case, if a propagation distance is very small, the bandwidth of a reconstruction point is equal to the maximum bandwidth of the SLM but only small portion of it contributes to reconstruction in consideration of Nyquist frequency. On the other hand, if a propagation distance becomes large enough, its bandwidth decreases in inverse proportion to the distance. Therefore, a quality metric increases within some distance and then it decreases. The distance to get a maximum quality metric is determined by sampling interval and total size of the SLM.

5.2. Issues

Even though digital holographic display is regarded as an ideal three-dimensional display, there still remain several issues to overcome. In this paper, we discuss some noteworthy ones out of these issues and introduce recent studies to solve these problems.

In digital holographic display, 3D view is reconstructed following the SBP, and the size of image and FOV is related with each other and their product is equal to the number of sampling in electro-optical modulators [85]. Since the optical wavelength in visible range is so small in comparison with the resolvable size by human eye, huge number of pixels in SLM is necessary to reconstruct digital holographic view volume with reasonable dimensions. For example, to reconstruct 350 mm by 350 mm image size holographic display with full parallax of FOV of 20 degrees, we need about 60 gigapixels in SLM. It is too huge number for implementation. Hence in digital holographic display, the technique to reduce the required number of pixels in SLM is one of the most important issues. Many studies have applied asymmetric optics to abandon vertical parallax and these approaches succeeded in decreasing the required SBP significantly. Therefore, HPO holography is regarded as a practical solution in current technology.

The image reconstructed from hologram generally has ‘speckle’ phenomenon, which appears as a high-contrast, fine-scale granular pattern. This phenomenon originates from interference of coherent light reflected from rough surfaces [86]. Since digital holography is based on the coherence of light, it is intrinsically inevitable. In speckle, the contrast naturally depends on the amount of coherence of light, and the fineness of granular pattern depends on the numerical aperture of a system. Therefore, to lessen this speckle phenomenon researchers tried to decrease the coherence of light and multiplex several images with speckle to obtain averaged intensity of them.

The ghost is also considered as undesirable phenomenon in digital holography. Originally, this word meant the convolution image between small fragment of object field and the whole object field [87]. Even though only one part of object field is used to reconstruct the hologram, the whole object field appears resulting from their convolution. But now this is frequently used to mean a noise which looks hazy in reconstruction image and sometimes it is used to describe autocorrelation or twin conjugate of a signal. This is expected to be solved by enhancing the quality of light source, optics, and their alignments.

Another practical problem in digital holography is recording dynamic objects. In real applications, it is not easy to record real object fields by an focal plane array (FPA) since the visibility of interference abruptly falls down when a movement of object is considerable in comparison of optical wavelength and exposure time of the FPA. Since there exists a limitation in reducing the exposure time, it is regarded as a more reasonable approach to use a pulse laser for recording in a short time [88]. In addition, the turbulence of the air which the object wave passes through also arises a problem for recording and there are many studies to correct this kind of aberration by an optimization algorithm [89]. In parallel, the methods to generate a hologram by computer have been deeply studied and the computation time has been remarkably reduced. Hence if the contents for digital holography are generated computationally, it is expected that there will be no significant obstruction to achieve it.

5.3. Status

Digital holographic display has been studied by many research groups and it is meaningful to introduce some remarkable systems. Stanley *et al*. presented 100 megapixel holographic display and they have a record as a system with the largest number of pixels [90]. This system is composed of 4 channels, where each channel has one electrically addressed (EA)

SLM and correspondent optically addressed (OA) SLMs. One EA SLM has 1 megapixels and distributes its information to twenty five OA SLMs sequentially. Hence one channel reconstructs an optical field with 25 megapixels and eventually the whole system has 100 megapixels. This system is designed to display images with 140 mm by 70 mm size and its horizontal FOV is 5.3 degrees.

Another possible approach is to form a view-window [91]. Instead of trying to enlarge the viewing angle which accompanies reduction of 3D image size or increase of SLM bandwidth requirement, view-window method generates small windows around the observer's eyes. 3D image is displayed such that it can be observed only through the window. Since each point of the 3D image is reconstructed only within narrow angular range, the SLM bandwidth requirement is much reduced. Although the narrow angular range results in some loss in the resolution of the displayed 3D image due to reduced effective numerical aperture (NA), the loss is not perceived by the observer since the reduced NA is still larger than that of the observer's eye. One drawback of this method is that the observer's position is fixed where the view-window is generated. Hence viewer tracking technology with an optical system to steer the location of the view-window is additionally required to enlarge effective viewing angle.

Figure 16 shows the principle of the view-window generation. With an SLM of around a few tens of micrometers pixel pitch which is currently available, the maximum diffraction angle is given under 1° or 2°. When a collimated laser illuminates the SLM in normal direction, each point on the SLM diffracts the incident light within this angular range in normal direction as shown in Fig. 16(a). By illuminating the SLM with a converging laser beam, the diffracted light converges, generating a view-window as shown in Fig. 16(b). The view-window size is given approximately by $2\theta d = d\lambda/\mathrm{p}$ where θ the diffraction angle, d view-window distance or focal

length of the lens for converging illumination, λ the wavelength, and p the pixel pitch of the SLM. For d=750 mm, λ=532 nm, and p=30 μm, the view-window size is 13.3 mm which can cover a single eye of the observer. When the observer locates his/her eye within this view-window, large size 3D image can be seen on whole SLM area. Therefore, in essence, the view-window method enlarges the 3D image size at the sacrifice of viewing angle for a given SLM bandwidth. Again the limitation in the viewing angle can be relieved by viewer tracking system.

In usual hologram, elementary hologram for each 3D image point covers whole area of the SLM. In the view-window method, however, the elementary hologram for each image point has limited SLM area due to narrow angular reconstruction range. This type of hologram is called sub-hologram. Figure 17 shows the concept of sub-hologram. Unlike the usual hologram shown in Fig. 17(a), the range of sub-hologram is limited to the area corresponding to the view-window as shown in Fig. 17(b). This reduced area contributes to the reduction of the computational load. In summary, the view-window method has advantage that large size 3D image can be displayed with currently available SLM. The requirement of the view-window steering system which is not easy to implement, however, is a drawback.

Using time-multiplexing, an interesting display system was proposed by Takaki's group [92]. It is implemented by a digital micro-mirror device (DMD). Since the DMD is a binary amplitude modulator, the undiffracted term originated from autocorrelation of a reference and the twin conjugate of a signal are optically filtered out. The aspect ratio of reconstructed image is determined by anamorphic imaging optics and imaging position is determined by a mechanical scanner. Since the DMD used as an SLM represents only binary information, reconstructed images are designed to be overlapped with each other to improve the quality of time-averaged view. Furthermore, this average is claimed helpful to reduce annoying speckle phenomenon.

5.4. Holography synthesis using integral imaging

Hologram recording of the real-existing objects has been studied for a few decades. By illuminating the object with a coherent light and interfering the object wave with a reference wave, the hologram of the object can be recorded. After advent of the digital holography which uses a CCD as a recording medium instead of holographic film, it has also been possible to extract the complex field of the object and apply digital processing [93]. This traditional method, however, requires well controlled laboratory environment for recording minute interference pattern. Hence it is not possible to capture hologram of a general 3D scene outside of the laboratory. This fact is especially severe limitation in the aspect of contents generation for holographic 3D displays.

Recently, active researches have been conducted to relieve this limitation. One approach is to synthesize hologram of the 3D scene from multiple perspective images captured under usual incoherent white illumination [94]. For a given 3D scene, a number of different perspectives are captured by either of camera array or moving camera system. The captured perspectives are processed considering corresponding ray directions with suitable phase factors to synthesize the hologram of the scene. Another approach is to use integral imaging [95, 96]. Instead of capturing multiple perspectives using complicated system, this method captures a set of elemental images of the 3D scene using a lens array under the integral imaging principle. The captured elemental images are processed to create a number of different sub-images of the 3D scene. Note that the sub-image has orthographic projection geometry where the projection lines are parallel. Considering this parallel projection geometry, the created sub-images are processed to synthesize the hologram of the captured 3D scene. Single capture process and parallel projection lines of integral imaging make the hologram synthesis process more efficient and precise. Figures 18(a)

and (b) show an example of the captured elemental images and the sub-images created from them. The hologram is synthesized using the created sub-images as shown in Fig. 18(c). Figure 18(d) shows numerical reconstruction results of the synthesized hologram at various distances. It can be observed that each object of a 3D scene is focused at different distance, convincing the 3D nature of the synthesized hologram. These methods using multiple perspectives or integral imaging enable to capture hologram of real-existing 3D scene in outdoor environment like usual 2D contents capture, which makes it feasible to generate contents for holographic 3D displays. However, the holograms synthesized by these methods have generally lower resolution than traditional holograms based on coherent interferometer, reserving large room for further enhancement.

5.5. Triangular-mesh based computer generated hologram

A synthesis algorithm of computer generated hologram (CGH) based on triangle-mesh model was introduced [97]. Usual standard software of 3D computer graphics produces triangulated mesh data for describing arbitrary 3D curved objects. An example of triangle mesh object is shown in Fig. 19. 3D volumetric object is basically composed of a closed set of triangles. In practice, for an observer at a specific observation position, a part of triangles in the full set of triangles of 3D object can be observed. According to this occlusion effect, the set of triangles can be divided into two distinct set of triangles; visible triangles and invisible triangles. This algorithmic problem is called visibility problem of 3D object.

The efficient solution of the visibility problem is provided by graphic card hardware. We can exploit the efficient and fast classification ability of graphic card hardware. In Figs. 20(a) and (b), the front view of 3D object and the partial set of visible triangles corresponding to the front view of the 3D object are presented, respectively. Invisible triangles are not drawn in Fig.

20(b). In Figs. 20(c) and (d), a different perspective view of the same 3D object and the corresponding set of visible triangles are presented. Graphic card supports almost real time processing for separating visible and invisible triangle groups.

The basic unit of CGH is the angular spectrum representation of a tilted triangle with arbitrary direction. After grouping the visible triangles of 3D object for a specific observation position, the angular spectrum representation of all visible triangles with their own tilt directions are computed and summed up coherently to produce complex 3D image light field. The mathematical model of the angular spectrum representation of tilted triangle has been developed in ref. [97]. In Fig. 21, a part of triangle-mesh surface with a diffusive surface that is represented by subdivided triangulation is shown. For a tilted triangle facet, the angular spectrum representation is firstly formulated in the local coordinate of the facet denoted by (x', y', z'), and then the angular spectrum is reformulated in the global coordinate system (x, y, z) by a rotational transformation. The diffusiveness or texture effect of a triangle facet can be realized by phase and amplitude encoding on subdivision triangles of a triangle facet.

In Figs. 22(a) and (b), A CGH synthesis setup and display setup are illustrated, respectively. In the configuration of optical Fourier transform, the light field radiated from the surface of 3D object is numerically recorded through a Fourier transform lens with a focal length of *f*. As a result, the CGH is equivalent to angular spectrum representation of visible surface of 3D object. The recorded angular spectrum CGH can be replayed by the same Fourier transform system, but the *x*-axis and *y*-axis must be inverted in the case of CGH display as shown in Fig. 22(b).

The recorded CGH is two-dimensional complex field distribution. Ideally, the complex modulator is necessary for modulation of both amplitude and phase profiles of an incident beam.

The complex modulator is particularly required for 3D holographic displays. Observation simulation results of holographic 3D image of the 3D model shown in Fig. 19 are presented in Fig. 23. Observers see the 3D holographic image at different depth planes. It is shown that th observed holographic object forms continuously curved surface along the optic axis.

The triangle-mesh based CGH synthesis algorithm provides very efficient and accurate holographic images of 3D objects with continuous spatial extent. With the advent of graphical processing unit (GPU), the efficient and fast computation of the angular spectrum of tilted triangle became possible. The computation efficiency can be exponentially enhanced with scalable implementation of multiple GPU computing machines.

6. See-through 3D display technologies

The ultimate goal of a 3D display may be generating a 3D image which is not distinguishable from real objects before we touch it. Of course, in the present status, the performance of 3D display in expressing 3D image is not good enough yet in reaching to the level of providing a realistic 3D image. However it is not enough just to raise the performance of a 3D display in order to meet the ultimate objective. For a seamless assimilation of 3D image into the real world, the display device should provide a see-through feature to mediate 3D image onto the real world, while the physical layout of the device is not noticeable to observers. Recently, augmented reality technology became an actively investigated research field that is to combine virtual and real physiological experiences [98, 99]. In augmenting visual sense of a user, the objective of augmented reality field is the same as the final goal of 3D display – providing perfect virtual image to the observer. In the early stage of augmented reality technology, a starting point of augmented reality display device was implementing a see-through display with 2D virtual images. However, with the development in the electronic and optical devices,

researches have been conducted on implementing a see-through display with 3D virtual images. In this section, we will overview some important recent reports on see-through 3D displays.

6.1. Head-mounted see-through display

Head-mounted display (HMD) is a very early type of see-through display that uses a display device attached just in front of a human eye [100]. Despite many disadvantages coming from head-worn requirement, it is still popular in some areas because of its easy and cheap implementation. Moreover, HMD can readily provide a 3D virtual image by a binocular disparity. Because of its long history, it is the most matured technique among augmented reality displays, and plenty of investigations have been conducted considering issues to be resolved. Nevertheless, further development is needed to commercialize see-through HMD devices. We will review some state of the art HMD techniques and efforts to resolve issues in implementing see-through HMD devices.

To implement a light-weighted and compact optical see-through HMD, it is preferred to adopt a wedge-shaped prism to fold the optical path of a displayed image to an observer [101,102]. Figure 24 shows a typical configuration of an optical see-through HMD using a wedge-shaped prism. A wedge-shaped prism labeled 1 guides the light from a display panel to show a virtual image to an observer. Three surfaces of a prism 1 are labeled *a*, *b* and *c* respectively as shown in Fig. 24. The surface *c* should be treated with a thin film coating that shows transreflective characteristic. The surfaces *b* and *c* are designed for total internal reflection (TIR) to occur at the surface *b* for the rays entered through the surface *a*. The reflected rays are reflected again at the surface *c* by a transreflective characteristic, so the brightness of an image is decreased to a certain degree by a reflectance of the surface *c*. The whole optical path of a displayed image through a prism 1 is depicted as a solid arrow in Fig. 24. The shape of three

surfaces should be designed to minimize the deformation of a displayed image shown to an observer. An auxiliary prism labeled 2 is attached to a wedge-shaped prism to achieve a see-through property of the system. If the surface *d* was properly designed, the deformation of an image passing through a wedge-shaped prism, caused by the refraction at the surfaces *b* and *c*, can be compensated by an auxiliary prism. The optical path of a transmitted see-through image is depicted as dashed arrows in Fig. 24. Because of a transreflective characteristic of the surface *c*, the brightness of the transmitted image is also affected by the transmittance of the surface *c*, and the transmittance should be determined considering applications and system specifications. With this configuration, a virtual image delivered to an observer by consecutive reflections inside a wedge-shaped prism can be overlaid on a real world scene shown through a combination of two prisms. Adopting freeform surface (FFS) provides a high degree of freedom in designing the shape of surfaces of prisms, so the deformation of a virtual image and a real world scene can be minimized. Cheng *et al*. introduced a systematic way to design surfaces of each prism using CODE V, and the result was verified by the prototype implementation using FFS prisms [103]. They reported achievement of a diagonal FOV of 53.5° and a *f*/# of 1.875, with an 8 mm exit pupil diameter and an 18.25 mm eye relief. Recently, they extended their work to provide wider FOV by tiling the system shown in Fig. 24 [104]. Figure 25 shows the concept of the tiled see-through HMD system. The surface shape of each prism is designed to have continuously cascaded FOV. Though the system needs a display device per each tiled prism, FOV can be easily widened to a level which is not achievable by tuning of one prism. They implemented the prototype with two FFS prisms tiled side by side, and the FOV of the prototype was widened to 82° × 32° with a small overlapping FOV to remove the vignetting effects at the transition region.

The optical see-through HMD using wedge-shaped prism shows that the entire system can be light-weighted and compact. However the optical path of a virtual image is usually on-axis when it enters the observer's pupil after consecutive reflections inside wedge-shaped prism. Instead of using such configuration, the tilted optical combiner that has optical power can be used to implement the off-axis configuration. Figure 26 shows layout of one of the state of the art systems with the off-axis configuration proposed by Zheng *et el*. [105]. Comparing with the on-axis configuration, the off-axis configuration has an advantage in that it can avoid the ghost image caused by multiple reflections inside the combiner.

One of the difficulties in mediating a virtual image to the real world with the optical see-through HMD is that a virtual image cannot occlude the real world when it is considered to be located between an observer and the real world scene. The usual way to resolve the occlusion problem is to adopt an active LC mask to block rays from the real world scene that coincides with a virtual image [106,107]. Kiyokawa *et al*. had conducted a series of work on implementing the optical see-through HMD free from such occlusion problem [108-111]. They also adopted an LC mask to selectively block the rays from the real world, but they concerned about a problem where the real world and the LC mask cannot be in focus simultaneously because of a large difference in their locations. To resolve such problem, the LC mask was located between symmetrically located two convex lenses with same specifications as shown in Fig. 27(a). With the configuration shown in Fig. 27(a), an image of the LC mask is located at infinity, so the LC mask and the real world scene are nearly in focus while the real world scene is maintained without lateral or transversal scaling. However there are some disadvantages in adopting a configuration shown in Fig. 27(a): The viewpoint of an observer is shifted by an offset of $2(f_{out} + f_{in})$. Hence the discomfort may arise by a mismatch between real and virtual viewpoints; The

upside-down image of real world scene is shown to the observer. In their recent work, Kiyokawa *et al*. implemented a ring-shaped system as shown in Fig. 27(b) to resolve these issues [111]. The rays from real world scene pass along a ring-shaped structure before shown to the observer, and the optical path is depicted as a solid arrow. The relay optics labeled 2 in Fig. 27(b) inverts the real world scene to compensate an upside down problem of a configuration in Fig. 27(a). Then the part of the system labeled 1, which is same as the configuration shown in Fig. 27(a), blocks selectively the rays from real world scene to provide a proper occlusion. A virtual image displayed on the display device is mediated to the masked real world image without an upside down problem by the optical combiner before reaching an observer. The ring-shaped structure shifts the virtual viewpoint of an observer to the location where an offset to the exit pupil of the system becomes the same as the real viewpoint, so the mismatch between the real and virtual viewpoints is also resolved. The investigation using the implemented prototype based on this configuration reported that more than 75% of people felt an enhanced sense of presence of virtual objects.

Most of the optical see-through HMDs simply combine a virtual image displayed on the display device which is usually located near an observer's eye. When a point of interest of an observer is at a distant object in the real world, the accommodation to a near virtual image and a distant real object has large difference, so it is difficult to provide a clear view of combined real and virtual images. Introducing vari-focal or multi-focal device for displaying a virtual image may resolve such a problem by shifting an image plane of a virtual image to a location where the point of interest of an observer is located [112,113]. The major problem in the vari-focal display is that it is usually implemented by a time-multiplexed mechanical motion, so the stability of a system is not guaranteed and even the flickering can occur in the displayed image. Another

approach to this issue is to project pixels of a virtual image directly on the retina of an observer's eye with a scanned laser beam [114]. However the quality of an image displayed by a scanning laser beam is not compatible yet to the ordinary display device. Recently Liu *et al*. had reported an interesting system which implements a vari-focal feature with an electronically controllable liquid lens [115]. In the implemented prototype, the liquid lens has a capability to vary optical power from -5 to 20 diopters by applying an AC voltage. Combined with a spherical mirror as shown in Fig. 28, a displayed virtual image can be shifted to provide focus cues continuously from optical infinity to as close as 8 diopters without any mechanical motion. However, if multiple virtual images with different locations are to be displayed, the liquid lens should address different optical powers simultaneously by time-multiplexing. The operating speed of the liquid lens is not so fast yet, so Liu *et al*. reported that their implementation could address two different focal planes up to the speed of 21.25 Hz which can cause a flickering to the HVS. Further developments in the electronic devices are required to address multiple focal planes without flickering. Hence it is still challenging to resolve the accommodation mismatch problem in the optical see-through HMDs.

6.2. Projection-type see-through 3D display technologies

Despite its long history, the see-through display based on HMD has many drawbacks that make it difficult to be accepted as a commercial product. Basically, the head-worn type limits the usage scenario significantly because the displayed contents can be delivered to only one user who wears the device. And the use in outdoor is also inconvenient because it is irrational to require users to always carry and wear the device when they want to enjoy the contents. Even the safety issues can arise from the heavy weight and limited FOV of the complicated structure. Hence HMD can be used only for very limited applications where the disadvantage of head-worn

type is not a big issue. Instead, the projection-type see-through display is considered as one viable candidate for implementing see-through display. The early implementation of projection-type see-through display was simply to adopt a large-sized optical combiner as a screen and to project a virtual image on the optical combiner [116]. A transreflective glass is the most popular option for the optical combiner because it shows clear see-through view of the real world scene. Though not much time had passed since the projection-type see-through display adopting a transreflective glass became a popular research topic, it is already in commercial market. Especially, the automobile industry is very active in adopting it as a head up display (HUD) on the windshield. Therefore the issues arisen from a non-flat transreflective glass are also explored in this area [117,118]. Sometimes a partially diffusive screen is also adopted for the optical combiner to enhance the FOV and brightness of a projected virtual image. Though it has a drawback that an image of the real world becomes blurred by a diffusive characteristic, it is sometimes preferred to a beam splitter because of wide viewing angle. Other than using a simple diffusive screen, some interesting ideas have been invented to implement a partially diffusive characteristic that can be used for an optical combiner [119-122]. One is an immaterial screen constructed by a flow of particles, such as dry fog, which is protected by a large non-turbulent airflow [119]. It is unique in that the observers can walk through the screen while the projected virtual image is well expressed by scattering of particles. The other one is to use water drops as a partially diffusive screen [120]. Because each water drop can be considered as a tiny fish eye lens, water drops shows scattering property for the projected image. The usefulness of these unique approaches have been investigated for various applications by many researchers [121,122]. We will review some recent technologies to implement a see-through 3D display based on the methods used for projection-type augmented reality displays.

The simplest way to implement a see-through display capable of providing 3D virtual image is to use transreflective glass to combine a 3D image from a conventional 3D display with a real world scene. One challenge in this configuration is that a real world scene is usually very far from the observer in many situations. Hence the adopted 3D display should be able to express a 3D image located far from the observer, but the ordinary autostereoscopic displays lack of providing such long distance 3D image. Takaki *et al*. introduced a super multi-view (SMV) display system for a 3D display in a see-through display to overcome such a problem [123]. SMV display is one kind of a multi-view display that limits the width of each viewing zone to be less than the diameter of eye pupil [124]. It is considered that a SMV display can provide an exact accommodation cue to a displayed 3D image and also a smooth motion parallax. Figure 29(a) shows a system configuration proposed by Takaki *et al*.. The SMV display was implemented by a combination of a slanted lenticular lens display and a projection lens. Though the application for a windshield display was assumed in their investigation, they used a flat transreflective mirror as an optical combiner to exclude the pre-warping issue in their considerations. As shown in Fig. 29(b), viewing zones of a slanted lenticular lens array is imaged by a projection lens and the width of the entire viewing zone is reduced. Hence the pitch of each viewing zone can be reduced to a desired level – less than a diameter of pupil of an eye – if parameters of the configuration were properly determined. Takaki *et al*. reported that their prototype provides 36 viewing zones with a pitch of 3.61 mm for each and is possible to demonstrate a continuous motion parallax for a 3D virtual image located from 5 m to 50 m far from the observer. Though the see-through display combining an ordinary 3D display with a real world scene by a transreflective mirror is intuitive and can express even the far virtual image with SMV configuration, the entire system is bulky and the size of displayed image is limited by

a size of the incorporated 3D display. Though it adopted a transreflective glass from a projection-type see-through display, it cannot be implemented as a projection-type. In the following subsections, we will introduce some 'projection-type' see-through 3D display based on a diffusive screen.

A projection-type see-through display adopting a diffusive screen basically has difficulty in providing 3D image because the image plane of a projected virtual image is fixed on a surface of the screen. Recently, Lee *et al*. proposed a system that introduces a depth-fused display (DFD) feature to show 3D image with a diffusive screen [125]. DFD is one of the 3D display techniques that can provide a 3D depth perception to an observer wearing no special apparatus with 2D images on overlapping two or more transparent screens – but generally two screens are enough [126]. An observer is restricted to be located at the position where identically rendered 2D images displayed on transparent screens are superimposed. Then the depth can be perceived pixel-by-pixel from superimposed 2D images by varying the luminance of each pixel of each 2D image. If a pixel on the frontal screen is more luminous, the pixel will be perceived to be near the observer. In contrast, if a pixel on the back screen is more luminous, the pixel will be perceived to be far from the observer. It is considered that an accommodation cue to fused depth perception is free from visual fatigue problems of stereoscopic displays [127]. Lee *et al*. adopted two FogScreens for diffusive screens, and they stacked two screens as shown in Fig. 30. They demonstrated that the superimposed two projected images can express a 3D volume in between two screens, and the fixed single viewpoint of DFD was overcome by using a head tracking. By using this technique, it is possible to implement a projection-type see-through display that can provide a 3D virtual image mediated to a real world. Even it is possible to walk through the screen because it is immaterial, and it can give a degree of freedom in a usage scenario. However,

the range where a 3D virtual image can be expressed is limited only between two screens, and the use of diffusive screen affects the quality of a real world scene.

One unique approach in implementing a projection-type see-through display with 3D virtual image is to use multiple water drop screens as diffusive screens proposed by Barnum *et al*. [128]. Instead of using DFD scheme, they tried to implement multiple image planes to express a virtual 3D image. Simply stacking multiple water drop screens cannot provide independent image planes because back plane image is diffused again by frontal diffusive screens. To address each image plane independently, time differential projection to each water drop screen is utilized. Unlike other diffusive screens, each particle of water drop screen moves continuously and is controllable. Hence it is possible to realize a time differential projection with a concept shown in Fig. 31. As shown in Fig. 31(a), if water drop from each drop emitter has slight time difference, it is possible to independently project water drop from each emitter with an obliquely located projector. If the projected image and the drop emitters were properly synchronized, water drops from each drop emitter can be addressed independently and the afterimage of water drops can show 2D image on each plane. In the implementation, Barnum *et al*. used a camera for the synchronization by calculating locations of drops from a captured image. With this implementation, they realized a system with independently addressable three water drop screens and 10 drops per second for each. Though they demonstrated only stacked 2D images, the DFD feature is readily applicable for each adjacent screen pair, so it is expected that the continuously expressed 3D virtual image can be successfully mediated with a real world scene by using this system. However this pioneering work is so sensitive to timing and alignment, so the further improvement is needed to resolve the stability issue as a commercial product.

6.3. See-through 3D display using holographic optical element

See-through display systems discussed so far demand optical combiners in any form to mediate a virtual image to a real world scene. The design and implementation of such an optical combiner is not easy, and sometimes it induces limitation in the performance of entire system. Holographic optical element (HOE) can be a good alternative to implement a required optical combiner in see-through display because holographic recording materials have many useful characteristics: it is ordinarily very clear and transparent even after an optical element is recorded; it is flexible, so there is high degree of freedom in designing a shape of system; it is very thin and lightweight. Though it is popular to adopt HOE for the optical see-through HMDs [129], we will investigate only the cases where HOE is applied to a projection-type see-through display system.

The difficulty in constructing a projection-type see-through display system using a diffusive screen was that the rays scattered on the diffusive screen lose the directivity, so left and right eyes cannot see different images. It means that there is no parallax in a displayed virtual image. HOE can be an alternative to an optical screen that can give a freely designed directivity to a projected image. Olwal *et al*. proposed an autotstereoscopic see-through system adopting an HOE as a screen that can show different virtual images to left and right eyes of an observer [130]. In their implementation as shown in Fig. 32, HOE is recorded to focus projected images from two projectors to different locations which are to be viewing zones for two eyes of an observer. If the viewing zones were properly designed, each eye of the observer views a virtual image coming from different projectors, and 3D image can be perceived by a binocular disparity. As a proof of concept, Olwal *et al*. implemented a system that has only two viewing zones with a HOE recorded on an ultra-fine grain silver-halide emulsion with a size of 30 cm × 40 cm. Therefore an autostereoscopic virtual image can only be viewed at a single fixed position and the

implemented system provides only monochrome image. Theoretically, the concept can be extended to a full-color multi-view system by recording HOE to have multiple viewing zones. However it will require multiple projectors that should be precisely aligned and the diffraction efficiency of HOE will decrease as the number of viewing zones increases. It will be worthy to verify a multi-view concept by a real implementation to check usability and limitation.

Takahashi *et al*. proposed an HOE that performs a lenticular-lens-like function in their series of works to show an autostereoscopic virtual image with a single projector [131-134]. Figure 33(a) shows a configuration of their proposed HOE structure which is composed of an array of identical grating cells. Each column of grating cell array coincides with each line of a lenticular lens. The concept of grating cell was adopted to increase a horizontal angular resolution at the cost of a decreased spatial resolution in vertical direction. Each grating cell is designed to diffract incident rays to 32 horizontal directions as shown in Fig. 33(b). Therefore the HOE can be considered as a lenticular lens that provides 32 multiple views in horizontal direction. To display a 3D virtual image using the recorded HOE, a properly calculated image is projected to the HOE and it is diffracted to 32 directions. In an observer's viewpoint, each grating cell of the HOE is recognized as one pixel of a displayed virtual image and the observer can view 32 different images changing viewing locations. Takahashi *et al*. also extended their work to realize a curved-lens-array-like configuration to increase the viewing angle of the system [134]. Implementing a physical optical structure that shows a curved lens array configuration results in a bulky system and a fabrication is usually difficult and expensive. However, it is possible to construct such feature as a flat and thin HOE because a direction of diffraction of each grating cell can be freely designed. When a center diffracted ray of each grating cell is designed to converge into a certain point in horizontal direction as shown in Fig. 33(c), the

desired characteristic can be implemented. Takahashi *et al*. reported that the viewing angle was increased from 42° to 74° by adopting such curved-lens-array-like feature.

6.4. See-through 3D display using concave half mirror array

Our group has recently proposed a new optical structure called a concave half mirror array (CHMA) whose external appearance is a transparent plate [135]. Inside a structure, there is an array of concave mirror with a transreflective characteristic as shown in Fig. 34. CHMA does not affect optical path of transmitted rays while the optical path of reflected rays are affected by a concave mirror array structure inside CHMA. Hence CHMA acts as different optical elements to reflected and transmitted light respectively. Figure 34 shows a system configuration that can implement a projection-type see-through 3D display based on CHMA. As CHMA is only a transparent plate to transmitted rays, it shows a see-through characteristic to a real world scene. Because a concave mirror array is a direct alternative to a lenslet array, a setup incorporating a projector can create a virtual 3D image by reflection of a projected elemental image. CHMA is the only possible method, except for HOE, that can mediate an autostereoscopic 3D image to a real world scene by a projection. The fabrication method presented in Ref. [135] is not appropriate for usage as see-through display because the implementation cannot be shown as a perfect transparent plate to transmitted rays. Hence the fabrication method should be further investigated to apply CHMA to a see-through 3D display.

7. Conclusion

It is hard to predict which one of outlined technologies will be the next to be a commercial product. Though the result completely depends on the demand of market, most of market researches forecast that autostereoscopic display and holography will be commercialized

in sequence. Those technologies can be categorized according to a principle laid under sampling and reconstruction process. As shown in Fig. 35, autostereoscopic display is a method to replicate a ray filed created by 3D objects. There are a set of digitized rays that an autosterescopic display can express and a ray field of 3D objects is sampled under that set of rays. The only difference between integral imaging and multi-view display such as lenticular lens exists in a sampling process. Integral imaging samples a ray field from ray source locations while multi-view display samples from predetermined viewpoints as compared in Fig. 35(a) and (b). Then such digitized ray field is reconstructed when an autostereoscopic display operates. Therefore autostereoscpic display is more appropriate to digital devices because various digital signal processing techniques developed so far can be applied directly. In contrast, holography is a technique to record and reconstruct wave field of a given 3D image and it shows a perfect reconstruction of 3D image in principle. However it is more difficult to represent an analog wave field with a digital display device, hence its implementation is considered more challenging than an autostereoscopic display.

Despite its easier implementation, autostereoscopy still needs further development in the display devices and optics because various quality factors of reconstructed ray field is severely limited by system parameters of display devices and optics. Representative quality factors of ray field are ray source resolution, angular sampling resolution and viewing angle as shown in Fig. 35(a). However, with the present status of display device and optics, a satisfactory 3D image is not reconstructed by an autostereoscopic display because only a part of ray field can be expressed.

See-through 3D display presents a mixture of ray field of both real world and virtual 3D image. It is more future technology and further development is needed to resolve some critical

issues. One important issue is an occlusion problem which was described in Sec. 6.1. Without appropriate occlusion of real world, reconstructed 3D image will suffer from a translucent problem. However, in dealing with 3D image, ray-based mask should be realized instead of a simple 2D mask. Hence it is needed to provide so called “occlusion field” in the real world side and no methods have been proposed to provide an occlusion field yet. If implemented, it may be similar with a ray field generation in principle. A difficulty in implementing a ray-based occlusion field is that there is the same limitation as in a ray-field based approach. It means that an occlusion field can address only a part of ray field from real world scene and it can affect a quality of real world scene. To avoid degradation in a real world scene, the occlusion field should cover sufficiently large part of ray field and it requires a further improvement in digital display devices than an autostereoscopic display.

In conclusion, it is still early to expect a commercial product based on autostereoscopic or holographic display devices. However we believe that a commercial product of them will appear in market shortly because technical issues discussed so far will be resolved in the end with continuing research effort and a value chain of 3D display industry is already working.

Acknowledgement

This work was supported by the National Research Foundation and the Ministry of Education, Science and Technology of Korea through the Creative Research Initiative Program (#2009-0063599).

References

1. C. Wheatstone, “Contributions to the physiology of vision.—Part the first. On some remarkable, and hitherto unobserved, phenomena of binocular vision,” Philos. Trans. R. Soc. London **128**, 371–394 (1838).
2. T. Inoue and H. Ohzu, “Accommodation responses to stereoscopic three-dimensional display,” Appl. Opt., vol. **36**, 4509-4515 (1997).
3. F. L. Kooi and A. Toet, “Visual comfort of binocular and 3D displays,” Displays, **25**, 99-108 (2004).
4. S. S. Kim, B. H. You, H. Choi, B. H. Berkeley, and N. D. Kim, “World's first 240Hz TFT-LCD technology for Full-HD LCD-TV and its application to 3D display,” SID Int. Sym. Digest Tech. Papers **40**, 424-427 (2009).
5. D.-S. Kim, S.-M. Park, J.-H. Jung, and D.-C. Hwang, “New 240Hz driving method for Full HD & high quality 3D LCD TV,” SID Int. Sym. Digest Tech. Papers **41**, 762-765 (2010).
6. H. Kang, S.-D. Roh, I.-S. Baik, H.-J. Jung, W.-N. Jeong, J.-K. Shin, and I.-J. Chung, “A novel polarizer glasses-type 3D displays with a patterned retarder,” SID Int. Sym. Digest Tech. Papers **41**, 1-4 (2010).
7. S.-M. Jung, Y.-B. Lee, H.-J. Park, S.-C. Lee, W.-N. Jeong, J.-K. Shin, I.-J. Chung, “Improvement of 3-D Crosstalk with Over-Driving Method for the Active Retarder 3-D Displays,” SID Int. Sym. Digest Tech. Papers, **41**, 1264-1267 (2010).
8. S. T. de Zwart, W. L. IJzerman, T. Dekker, and W. A. M. Wolter, “A 20-in. switchable auto-stereoscopic 2D/3D display,” *in Proceedings of International Display Workshops*, 1459-1460 (2004).

9. G. J. Woodgate and J. Harrold, “A new architecture for high resolution autostereoscopic 2D/3D displays using free-standing liquid crystal microlenses,” SID Int. Symp. Digest Tech. Papers **36**, 378-381 (2005).
10. H.-K. Hong, S.-M. Jung, B.-J. Lee, H.-J. Im, and H.-H. Shin, “Autostereoscopic 2D/3D switching display using electric-field-driven LC lens (ELC lens),” SID Int. Sym. Digest Tech. Papers **39**, 348-351 (2008).
11. C.-W. Chen, Y.-C. Huang, Y.-P. Huang, “Fast switching Fresnel liquid crystal lens for autostereoscopic 2D/3D display,” SID Int. Sym. Digest Tech. Papers **41**, 428-431 (2010).
12. A. Takagi, T. Saishu, M. Kashiwagi, K. Taira, and Y. Hirayama, “Autostereoscopic partial 2-D/3-D switchable display using liquid-crystal gradient index lens,” SID Int. Sym. Digest Tech. Papers **41**, 436-439 (2010).
13. H. J. Lee, H. Nam, J. D. Lee, H. W. Jang, M. S. Song, B. S. Kim, J. S. Gu, C. Y. Park, and K. H. Choi, “A high resolution autostereoscopic display employing a time division parallax barrier,” SID Int. Symp. Digest Tech. Papers **37**, 81-84 (2006).
14. G. Hamagishi, “Analysis and improvement of viewing conditions for two-view and multi-view 3D displays,” SID Int. Symp. Digest Tech. Papers **40**, 340-343 (2009).
15. G. Lippmann, “La photographie integrale,” C. R. Acad, Sci. **146**, 446-451 (1908).
16. F. Okano, H. Hoshino, J. Arai, and I. Yuyama, “Real-time pickup method for a three-dimensional image based on integral photography,” Appl. Opt. **36**, 1598-1603 (1997).
17. B. Lee, J.-H. Park, and S.-W. Min, “Three-dimensional display and information processing based on integral imaging,” in Digital Holography and Three-Dimensional Display (edited by T.-C. Poon), Springer, New York, USA, 2006, Chapter 12, pp. 333-378.

18. S.-W. Min, J. Kim, and B. Lee, "New characteristic equation of three-dimensional integral imaging system and its applications," Jpn. J. appl. Phys. **44**, L71-L74 (2005).
19. J.-H. Park, K. Hong, and B. Lee, "Recent progress in three-dimensional information processing based on integral imaging," Appl. Opt. **48**, H77-H94 (2009).
20. Y. Kim, S.-g. Park, S.-W. Min, and B. Lee, "Integral imaging system using a dual-mode technique," Appl. Opt. **48**, H71-H76 (2009).
21. J. Hahn, Y. Kim, and B. Lee, "Uniform angular resolution integral imaging display with boundary folding mirrors," Appl. Opt. 48, 504-511 (2009).
22. Y. Takaki, K. Tanaka, and J. Nakamura, "Super multi-view display with a lower resolution flat-panel display," Opt. Express **19**, 4129-4139 (2011).
23. M. Okui, M. Kobayashi, J. Arai, and F. Okano, "Moire fringe reduction by optical filters in integral three-dimensional imaging on a color flat-panel display," Appl. Opt. 44, 4475-4483 (2005).
24. Y. Kim, G. Park, J.-H. Jung, J. Kim, and B. Lee, "Color moire pattern simulation and analysis in three-dimensional integral imaging for finding the moire-reduced tilted angle of a lens array," Appl. Opt. 48, 2178-2187 (2009).
25. Y. Kim, S.-g. Park, S.-W. Min, and B. Lee, "Projection-type integral imaging system using multiple elemental image layers," Appl. Opt. **50**, B18-B24 (2011).
26. M. Kawakita, H. Sasaki, J. Arai, F. Okano, K. Suehiro, Y. Haino, M. Yoshimura, and M. Sato, "Geometric analysis of spatial distortion in projection-type integral imaging," Opt. Lett. **33**, 684-686 (2008).
27. F. Okano, J. Arai, and M. Kawakita, "Wave optical analysis of integral method for three-dimensional images," Opt. Lett. **32**, 364-366 (2007).

28. X. Wang and H. Hua, "Theoretical analysis for integral imaging performance based on microscanning of a microlens array," Opt. Lett. **33**, 449-451 (2008).
29. J.-S. Jang and B. Javidi, "Improved viewing resolution of three-dimensional integral imaging by use of nonstationary micro-optics," Opt. Lett. **27**, 324-326 (2002).
30. H. Choi, S.-W. Min, S. Jung, J.-H. Park, and B. Lee, "Multiple-viewing-zone integral imaging using a dynamic barrier array for three-dimensional displays," Opt. Express **11**, 927-932 (2003).
31. B. Lee, S. Jung, and J.-H. Park, "Viewing-angle-enhanced integral imaging by lens switching," Opt. Lett. **27**, 818-820 (2002).
32. J.-S. Jang and B. Javidi, "Improvement of viewing angle in integral imaging by use of moving lenslet arrays with low fill factor," Appl. Opt. **42**, 1996-2002 (2003).
33. S. Jung, J.-H. Park, H. Choi, and B. Lee, "Wide-viewing integral three-dimensional imaging by use of orthogonal polarization switching," Appl. Opt. **42**, 2513-2520 (2003).
34. G. Park, J.-H. Jung, K. Hong, Y. Kim, Y.-H. Kim, S.-W. Min, and B. Lee, "Multi-viewer tracking integral imaging system and its viewing zone analysis," Opt. Express **17**, 17895-17908 (2009).
35. Y. Kim, J.-H. Park, S.-W. Min, S. Jung, H. Choi, and B. Lee, "A wide-viewing-angle integral 3D imaging system by curving a screen and a lens array," Appl. Opt. **44**, 546-552 (2005).
36. Y. Kim, J.-H. Park, H. Choi, S. Jung, S.-W. Min, and B. Lee, "Viewing-angle-enhanced integral imaging system using a curved lens array," Opt. Express **12**, 421-429 (2004).
37. D.-H. Shin, B. Lee, and E.-S. Kim, "Multidirectional curved integral imaging with large depth by additional use of a large-aperture lens," Appl. Opt. **4**5, 7375-7381 (2006).

38. J.-H. Jung, K. Hong, G. Park, I. Chung, and B. Lee, "360-degree viewable cylindrical integral imaging system using three-dimensional/two-dimensional switchable and flexible backlight," J. Soc. Inf. Display **18**, 527-534 (2010).
39. S.-W. Min, J. Kim, and B. Lee, "Wide-viewing projection-type integral imaging system with an embossed screen," Opt. Lett. **29**, 2420-2422 (2004).
40. R. Martinez-Cuenca, H. Navarro, G. Saavedra, B. Javidi, and M. Martinez-Corral, "Enhanced viewing-angle integral imaging by multiple-axis telecentric relay system," Opt. Express **15**, 16255-16260 (2007).
41. G. Baasantseren, J.-H. Park, K.-C. Kwon, and N. Kim, "Viewing angle enhanced integral imaging display using two elemental image masks," Opt. Express **17**, 14405-14417 (2009).
42. H. Kim, J. Hahn, and B. Lee, "The use of a negative index planoconcave lens array for wide-viewing angle integral imaging," Opt. Express **16**, 21865-21880 (2008).
43. J.-Y. Jang, H.-S. Lee, S. Cha, and S.-H. Shin, "Viewing angle enhanced integral imaging display by using a high refractive index medium," Appl. Opt. **50**, B71-B76, 2011.
44. H. Liao, T. Dohi, and M. Iwahara, "Improved viewing resolution of integral videography by use of rotated prism sheets," Opt. Express **15**, 4814-4822 (2007).
45. Y. Kim, J. Kim, J.-M, Kang, J.-H. Jung, H. Choi, and B. Lee, "Point light source integral imaging with improved resolution and viewing angle by the use of electrically movable pinhole array," Opt. Express **15**, 18253-18267 (2007).
46. H. Liao, M. Iwahara, N. Hata, and T. Dohi, "High-quality integral videography using a multiprojector," Opt. Express **12**, 1067-1076 (2004).

47. H. Liao, M. Iwahara, T. Koike, N. Hata, I. Sakuma, and T. Dohi, "Scalable high-resolution integral videography autostereoscopic display with a seamless multiprojection system," Appl. Opt. **44**, 305-315 (2005).
48. J.-S. Jang, F. Jin, and B. Javidi, "Three-dimensional integral imaging with large depth of focus by use of real and virtual image fields," Opt. Lett. **28**, 1421-1423 (2003).
49. J.-H. Park, S. Jung, H. Choi, and B. Lee, "Integral imaging with multiple image planes using a uniaxial crystal plate," Opt. Express **11**, 1862-1875 (2003).
50. J.-S. Jang and B. Javidi, "Large depth-of-focus time-multiplexed three-dimensional integral imaging by use of lenslet with nonuniform focal lengths and aperture sizes," Opt. Lett. **28**, 1924-1926 (2003).
51. H. Choi, J.-H. Park, J. Hong, and B. Lee, "Depth enhanced integral imaging with a stepped lens array or a composite lens array for three-dimensional display," Jpn. J. Appl. Phys. **43**, 5330-5336 (2004).
52. S. Jung. J. Hong, J.-H. Park, Y. Kim, and B. Lee, "Depth-enhanced integral-imaging 3D display using different optical path lengths by polarization devices or mirror barrier array," J. Soc. Inf. Display **12**, 461-467 (2004).
53. J. Hong, J.-H. Park, S. Jung, and B. Lee, "Depth enhanced integral imaging by use of optical path control," Opt. Lett. **29**, 1790-1792 (2004).
54. H. Choi, Y. Kim, J.-H. Park, J. Kim, S.-W. Cho, and B. Lee, "Layered-panel integral imaging without the translucent problem," Opt. Express **13**, 5769-5776 (2005).
55. Y. Kim, J.-H. Park, H. Choi, J. Kim, S.-W. Cho, Y. Kim, G. Park, and B. Lee, "Depth-enhanced integral imaging display system with electrically variable image planes using polymer-dispersed liquid-crystal layers," Appl. Opt. **46**, 3766-3773 (2007).

56. S.-W. Min, M. Hahn, J. Kim, and B. Lee, "Three-dimensional electro-floating display system using an integral imaging method," Opt. Express **13**, 4358-4369 (2005).
57. J. Kim, S.-W. Min, Y. Kim, and B. Lee, "Analysis on viewing characteristics of integral floating system," Appl. Opt. **47**, D80-D86 (2008).
58. J. Kim, S.-W. Min, and B. Lee, "Viewing window expansion of integral floating display," Appl. Opt. **48**, 862-867 (2009).
59. J. Kim, S.-W. Min, and B. Lee, "Viewing region maximization of an integral floating display through location adjustment of viewing window," Opt. Express **15**, 13023-13034 (2007).
60. J. Kim, S.-W. Min, and B. Lee, "Floated image mapping for integral floating display," Opt. Express **16**, 8549-8556 (2008).
61. H. Kakeya, "Autostereoscopic display with real-image virtual screen and light filters," Proc. SPIE **4660**, 349-357 (2002).
62. H. Kakeya, "MOEVsion: simple multiview display with clear floating image," Proc. SPIE **6490**, 64900J (2007).
63. H. Choi, Y. Kim, J. Kim, S.-W. Cho, and B. Lee, "Depth- and viewing-angle-enhanced 3-D/2-D switchable display system with high contrast ratio using multiple display devices and a lens array," J. Soc. Inf. Display **15**, 315-320 (2007).
64. Y. Kim, H. Choi, J. Kim, S.-W. Cho, Y. Kim, G. Park, and B. Lee, "Depth-enhanced integral imaging display system with electrically variable image planes using polymer-dispersed liquid crystal layers," Appl. Opt. **46**, 3766-3773 (2007).
65. H. Choi, S.-W. Cho, J. Kim, and B. Lee, "A thin 3D-2D convertible integral imaging system using a pinhole array on a polarizer," Opt. Express **14**, 5183-5190 (2006).

66. S.-W. Cho, J.-H. Park, Y. Kim, H. Choi, J. Kim, and B. Lee, "Convertible two-dimensional-three-dimensional display using an LED array based on modified integral imaging," Opt. Lett. **31**, 2852-2854 (2006).

67. Y. Kim, H. Choi, S.-W. Cho, Y. Kim, J. Kim, G. Park, and B. Lee, "Three-dimensional integral display using plastic optical fibers," Appl. Opt. **46**, 7149-7154 (2007).

68. Y. Kim, J. Kim, Y. Kim, H. Choi, J.-H. Jung, and B. Lee, "Thin-type integral imaging method with an organic light emitting diode panel," Appl. Opt. **47**, 4927-4934 (2008).

69. J.-H. Jung, Y. Kim, Y. Kim, J. Kim, K. Hong, and B. Lee, "Integral imaging system using an electroluminescent film backlight for three-dimensional-two-dimensional convertibility and a curved structure," Appl. Opt. **48**, 998-1007 (2009).

70. H. Choi, J. Kim, S.-W. Cho, Y. Kim, J. B. Park, and B. Lee, "Three-dimensional-two-dimensional mixed display system using integral imaging with an active pinhole array on a liquid crystal panel," Appl. Opt. **47**, 2207-2214 (2008).

71. D. Gabor, "A new microscopic principle," Nature **161**, 777–778 (1948).

72. E. N. Leith and J. Upatnieks, "Reconstructed wavefronts and communication theory," J. Opt. Soc. Am. **52**, 1123–1130 (1962).

73. Y. N. Denisyuk, "Photographic reconstruction of the optical properties of an object in its own scattered field," Sov. Phys. Dokl. **7**, 543 (1962).

74. G. Lippmann, "La photographie des couleurs," C.R. Hebd. Acad. Sci. **112**, 274–275 (1891).

75. A. W. Lohmann and D. Paris, "Binary Fraunhofer holograms generated by computer," Appl. Opt. **6**, 1739–1748 (1967).

76. J. W. Goodman and R. W. Lawrence, "Digital image formation from electronically detected holograms," Appl. Phys. Lett. **11**, 77–79 (1967).

77. J. Schmit and K. Creath, "Extended averaging technique for derivation of error-compensating algorithms in phase-shifting interferometry," Appl. Opt. **34**, 3610-3619 (1995).

78. I. Yamaguchi and T. Zhang, "Phase-shifting digital holography," Opt. Lett. **22**, 1268-1270 (1997).

79. J. Millerd, N. Brock, J. Hayes, M. North-Morris, M. Novak, and J. C. Wyant, "Pixelated phase-mask dynamic interferometer," in Proc. SPIE **5531**, 304-314 (2004).

80. J. W. Goodman, *Introduction to Fourier Optics*, 3rd ed. (Roberts & Company Publishers, 2004).

81. A. V. Oppenheim and J. S. Lim, "The importance of phase in signals," Proceedings of the IEEE **69**, 529-541 (1981).

82. J. Hahn, H. Kim, Y. Lim, G. Park, and B. Lee, "Wide viewing angle dynamic holographic stereogram with a curved array of spatial light modulators," Opt. Express **16**, 12372-12386 (2008).

83. D. J. Brady, Optical Imaging and Spectroscopy, (Wiley, 2009).

84. L. Onural, F. Yaraş, and H. Kang, "Digital holographic three-dimensional video displays," Proc. of the IEEE **99**, 576-589 (2011).

85. K. Maeno, N. Fukaya, O. Nishikawa, K. Sato, and T. Honda, "Electro-holographic display using 15 mega pixels LCD," Proc. SPIE **2652**, 15-23 (1996).

86. J. W. Goodman, Speckle Phenomena in Optics: Theory and Applications, (Roberts & Company, 2007).

87. P. J. van Heerden, "A New Optical Method of Storing and Retrieving Information," Appl. Opt. 2, 387-392 (1963).

88. N. Abramson, "Light-in-flight recording: high-speed holographic motion pictures of ultrafast phenomena," Appl. Opt. **22**, 215-232 (1983).

89. J. R. Fienup and J. J. Miller, "Aberration correction by maximizing generalized sharpness metrics," J. Opt. Soc. Am. A **20**, 609-620 (2003).

90. M. Stanley, R. W. Bannister, C. D. Cameron, S. D. Coomber, I. G. Cresswell, J. R. Hughes, V. Hui, P. O. Jackson, K. A. Milham, R. J. Miller, D. A. Payne, J. Quarrel, D. C. Scattergood, A. P. Smith, M. A. Smith, D. L. Tipton, P. J. Watson, P. J. Webber, and C. W. Slinger, "100 mega-pixel computer generated holographic images from active tiling--a dynamic and scalable electro-optic modulator system," Proc. SPIE **5005**, 247-258 (2003).

91. R. Haussler, S. Reichelt, N. Leister, E. Zschau, R. Missbach, and A. Schwerdtner, "Large real-time holographic displays: from prototypes to a consumer product," Proc. SPIE **7237**, 72370S (2009).

92. Y. Takaki and M. Yokouchi, "Speckle-free and grayscale hologram reconstruction using time-multiplexing technique," Opt. Express **19**, 7567-7579 (2011).

93. I. Yamaguchi and T. Zhang, "Phase-shifting digital holography," Opt. Lett. **22**, 1268-1270 (1997).

94. N.T. Shaked, B. Katz, and J. Rosen, "Review of three-dimensional holographic imaging by multiple-viewpoint-projection based methods," Appl. Opt. **48**, H120–-H136 (2009).

95. J.-H. Park, M.-S. Kim, G. Baasantseren, and N. Kim, "Fresnel and Fourier hologram generation using orthographic projection images,"Opt. Express **17**, 6320-6334 (2009).

96. N. Chen, J.-H. Park, and N. Kim, "Parameter analysis of integral Fourier hologram and its resolution enhancement," Opt. Express **18**, 2152-2167 (2010).

97. H. Kim, J. Hahn, and B. Lee, "Mathematical modeling of triangle-mesh-modeled three-dimensional surface objects for digital holography," Appl. Opt. **47**, D117-D127 (2008).

98. F. Zhou, H. B.-L. Duh, and M. Billinghurst, "Trends in augmented reality tracking, interaction and display: A review of ten years of ISMAR," *in Proceedings of 7th IEEE/ACM International Symposium* (IEEE, 2008), pp. 193.

99. D. W. F. van Krevelen and R. Poelman, "A Survey of Augmented Reality Technologies, Applications and Limitations," Int. J. Virtual Reality, **9**, 1-20 (2010).

100. O. Cakmakci and J. Rolland, "Head-worn displays: a review," J. Disp. Technol. **2**, 199-216 (2006).

101. H. Morishima, T. Akiyama, N. Nanba, and T. Tanaka, "The design of off-axial optical system consisting of aspherical mirrors without rotational symmetry," in 20th Optical Symposium, Extended Abstracts, **21**, 53-56 (1995).

102. K. Inoguchi, H. Morishima, N. Nanaba, S. Takeshita, and Y. Yamazaki, "Fabrication and evaluation of HMD optical system consisting of aspherical mirrors without rotation symmetry," in Japan Optics'95, Extended Abstracts, 19–20 (1995).

103. D. Cheng, Y. Wang, H. Hua, and M. M. Talha, "Design of an optical see-through head-mounted display with a low f-number and large field of view using a freeform prism," Appl. Opt. **48**, 2655-2668 (2009).

104. D. Cheng, Y. Wang, H. Hua, and J. Sasian, "Design of a wide-angle, lightweight head-mounted display using free-form optics tiling," Opt. Lett. **36**, 2098-2100 (2011).

105. Z. Zheng, X. Liu, H. Li, and L. Xu, "Design and fabrication of an off-axis see-through head-mounted display with an x–y polynomial surface," Appl. Opt. **49**, 3661-3668 (2010).

106. E. W. Tatham, “Technical opinion: getting the best of both real and virtual worlds,” Commun. ACM. **42**, 96-98 (1999).

107. O. Cakmakci, Y. Ha, and J. P. Rolland, “A Compact Optical See-Through Head-Worn Display with Occlusion Support,” *in Proceedings of the 3rd IEEE/ACM International Symposium on Mixed and Augmented Reality* (IEEE/ACM, 2004), pp. 16-25.

108. K. Kiyokawa, Y. Kurata, and H. Ohno, “An Optical See-through Display for Mutual Occlusion with a Real-time Stereo Vision System,” Computer & Graphics **25**, pp. 765-779 (2001).

109. K. Kiyokawa, Y. Kurata, and H. Ohno, “Occlusive Optical See-through Displays in a Collaborative Setup,” *in Proceedings of the ACM SIGGRAPH* (ACM 2002), p.74.

110. K. Kiyokawa, M. Billinghurst, S. E. Hayes, A. Gupta, Y. Sannohe, and H. Kato, “Communications Behaviors of Co-located Users in Collaborative AR Interfaces,” *in Proceedings of the IEEE/ACM International Symposium on Mixed and Augmented Reality* (IEEE/ACM 2002), pp.139-148.

111. K. Kiyokawa, M. Billinghurst, B. Campbell, and E. Woods, “An Occlusion-Capable Optical See-through Head Mount Display for Supporting Co-located Collaboration,” *in Proceedings of the 2nd IEEE/ACM International Symposium on Mixed and Augmented Reality* (IEEE/ACM 2003), pp.133.

112. S. Shiwa, K. Omura, and F. Kishino, “Proposal for a 3-D Display with Accommodative Compensation: 3-DDAC,” J. Soc. Inf. Display, **4**, 255-261 (1996).

113. T. Shibata, T. Kawai, K. Ohta, M. Otsuki, N. Miyake, Y. Yoshihara, and T. Iwasaki, “Stereoscopic 3-D Display with Optical Correction for the Reduction of the Discrepancy between Accommodation and Convergence,” J. Soc. Inf. Display, **13**, 665-671 (2005).

114. S.C. McQuaide, E.J. Seibel, J.P. Kelly, B.T. Schowengerdt, and T.A.A. Furness, "A Retinal Scanning Display System That Produces Multiple Focal Planes with a Deformable Membrane Mirror," Displays, **24**, 65-72 (2003).

115. S. Liu, H. Hua, and D. Cheng, "A Novel Prototype for an Optical See-Through Head-Mounted Display with Addressable Focus Cues," IEEE Trans. Vis. Comput. Graph. **16**, 381-393 (2010).

116. A. Olwal and T. Höllerer. "POLAR: portable, optical see-through, low-cost augmented reality," *in Proceedings of the ACM symposium on Virtual reality software and technology* (ACM, 2005), pp. 227-230.

117. W. Wu, F. Blaicher, J. Yang, T. Seder, and D. Cui, "A prototype of landmark-based car navigation using a full-windshield head-up display system," *in Proceedings of the 2009 workshop on Ambient media computing* (AMC 2009), pp. 21-28.

118. A. Sato, I. Kitahara, K. Yoshinari, and O. Yuichi, "Visual navigation system on windshield head-up display," *in Proceedings of 13th world congress & exhibition on intelligent transport systems and services* (2006).

119. K. Palovuori, I. Rakkolainen. Method and apparatus for forming a projection screen or a projection volume. U.S. patent 6819487. Nov. 16, 2004.

120. S. Eitoku, K. Nishimura, T. Tanikawa, and M. Hirose, "Study on design of controllable particle display using water drops suitable for light environment," *in Proceeding of the ACM Symposium on Virtual Reality Software and Technology* (ACM, 2009), pp. 23-26.

121. A. Olwal, S. DiVerdi, N. Candussi, I. Rakkolainen, and T. Hollerer, "An Immaterial, Dual-sided Display System with 3D Interaction," *in Proceedings of the IEEE conference on Virtual Reality* (IEEE 2006), pp.279-280.

122. S. DiVerdi, I. Rakkolainen, T. Höllerer, and A. Olwal, “A Novel Walk-Through 3D Display,” Proc. SPIE **6055**, 605519 (2006).

123. Y. Takaki, Y. Urano, S. Kashiwada, H. Ando, and K. Nakamura, "Super multi-view windshield display for long-distance image information presentation," Opt. Express **19**, 704-716 (2011).

124. Y. Takaki and N. Nago, “Multi-projection of lenticular displays to construct a 256-view super multi-view display,” Opt. Express **18**, 8824–8835 (2010).

125. C. Lee, S. DiVerdi, and T. Ho¨ llerer, “Depth-Fused 3-D Imagery on an Immaterial Display,” IEEE Trans. Vis. and Comput. Graph. **15**, 20-32, (2009).

126. S. Suyama, Y. Ishigure, H. Takada, K. Nakazawa, J. Hosohata, Y. Takao, and T. Fujikao, “Apparent 3-D Image Perceived from Luminance-Modulated Two 2-D Images Displayed at Different Depths,” Vision Res. **44**, 785-793 (2004).

127. Y. Ishigure, S. Suyama, H. Takada, K. Nakazawa, J. Hosohata, Y. Takao, and T. Fujikado, “Evaluation of Visual Fatigue Relative in the Viewing of a Depth-Fused 3D Display and 2D Display,” *in Proceeding of International Display Workshops* (2004).

128. P. C. Barnum, S. G. Narasimhan, and T. Kanade, “A multi-layered display with water drops,” ACM Trans. Graph. **29**, Article 76 (2010).

129. I. Kasai, Y. Tanijiri, T. Endo, and H. Ueda, “A Practical See-Through Head Mounted Display Using a Holographic Optical Element,” Opt. Rev. **8**, 241-244 (2001).

130. Alex Olwal, Jonny Gustafsson and Christoffer Lindfors, "Spatial augmented reality on industrial CNC-machines", Proc. SPIE **6804**, 680409 (2008).

131. K. Sakamoto, M. Okamoto, H. Ueda, H. Takahashi, and E. Shimizu, "Real-time 3D color display using a holographic optical element", Proc. SPIE **2652**, 124-131 (1996).

132. K. Sakamoto, H. Takahashi, E. Shimizu, H. Ueda, K. Tanaka, and M. Okamoto, "New approach to the real-time 3D display using a holographic optical element", Proc. SPIE **3011**, 36-44 (1997).

133. R. Kishigami, H. Takahashi, and E. Shimizu, "Real-time color three-dimensional display system using holographic optical elements", Proc. SPIE **4296**, 102-107 (2001).

134. H. Takahashi, H. Fujinami, and K. Yamada, "Wide-viewing-angle three-dimensional display system using HOE lens array", Proc. SPIE **6055**, 60551C (2006).

135. J. Hong, Y. Kim, S. Park, J.-H. Hong, S.-W. Min, S.-D. Lee, and B. Lee, "3D/2D convertible projection-type integral imaging using concave half mirror array," Opt. Express **18**, 20628-20637 (2010).

Figure captions

Fig.1. Number of search results from Google Scholar (http://scholar.google.com). Searching was restricted only to title of papers. Queries for each technology were ‘stereoscopy or stereoscopic,’ ‘integral imaging,’ ‘lenticular lens,’ and ‘parallax barrier’ respectively. Numbers in 2011 are estimations based on the results obtained on July 2011.

Fig.2. Depth cues associated with 3D information: (a) psychological cues, (b) physiological cues

Fig.3. Principle of stereoscopic 3D display with LC shutter glasses

Fig.4. The structure and principle of PR technology

Fig.5. The structure and principle of AR or SIP technology

Fig.6. The principle and structure of 3-view lenticular lens 3D display

Fig.7. Operations of 2D/3D convertible lenticular lens display using patterned electrode method: (a) 3D mode (b) 2D mode.

Fig.8. Operation of 2D/3D convertible parallax barrier display using LC panel: (a) 3D mode (b) 2D mode

Fig.9. The structure and concept of integral imaging

Fig.10. Display modes of integral imaging: (a) focal display mode, (b) real/virtual display mode, and (c) simulation results of reconstructed 3D image in focal display mode and real/virtual display mode. For the simulation of focal display mode, 1 mm × 1 mm lens array with focal length of 3 mm was assumed. For the real/virtual mode, 10 mm × 10 mm lens array with focal length of 30 mm was assumed and the central depth planed is located 90 mm in front of lens array. Pixel pitch of display is 0.08 mm × 0.08 mm for both cases. In this figure, distortion of reconstructed image at two locations out from in-focus plane is compared. In

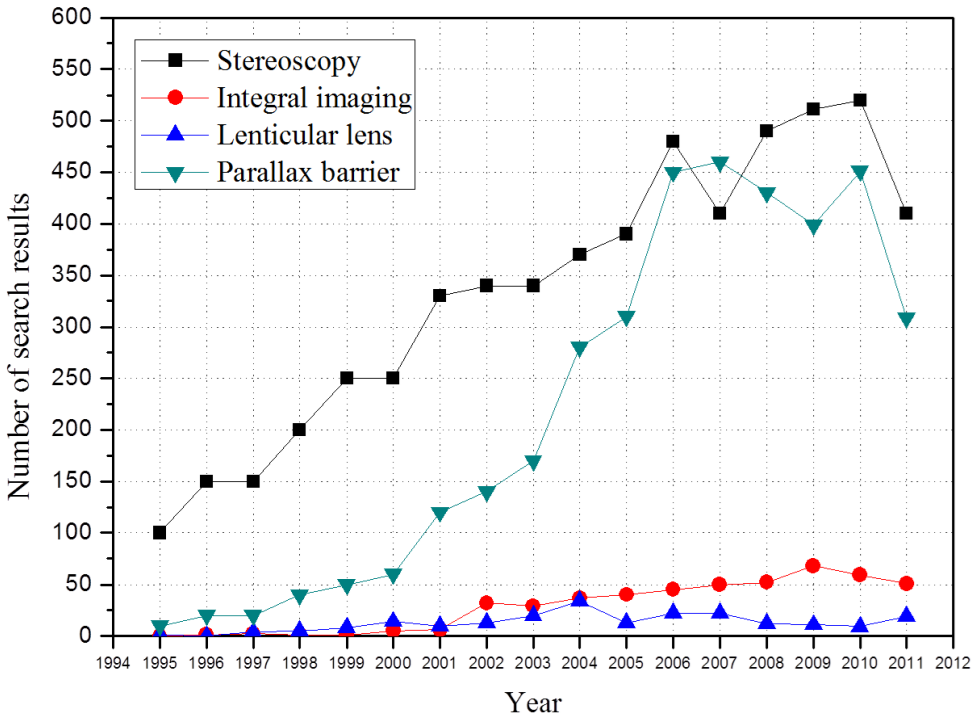
Stereoscopy
Integral imaging
Lenticular lens
Parallax barrier
Number of search results
Year
0
50
100
150
200
250
300
350
400
450
500
550
600
1994
1995
1996
1997
1998
1999
2000
2001
2002
2003
2004
2005
2006
2007
2008
2009
2010
2011
2012

Fig. 1.

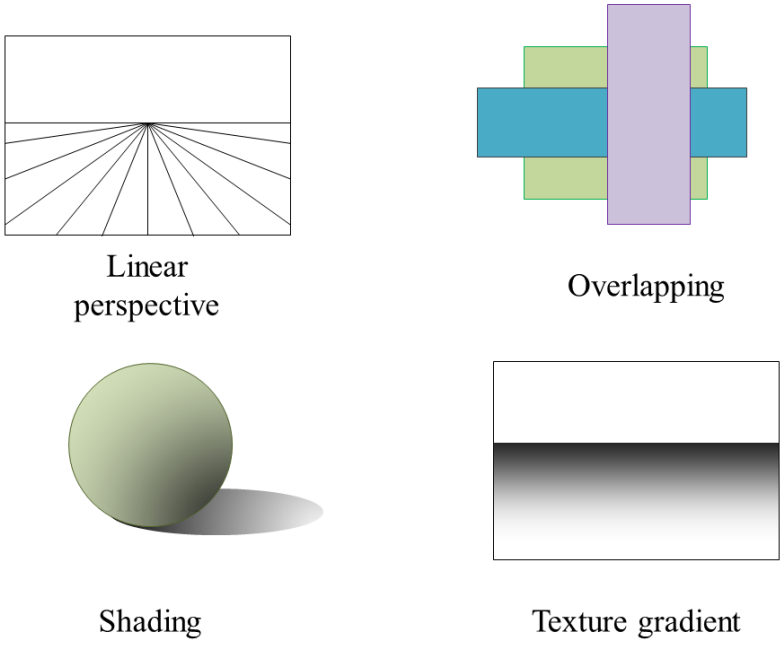
Linear
perspective
Overlapping
Shading
Texture gradient

(a)

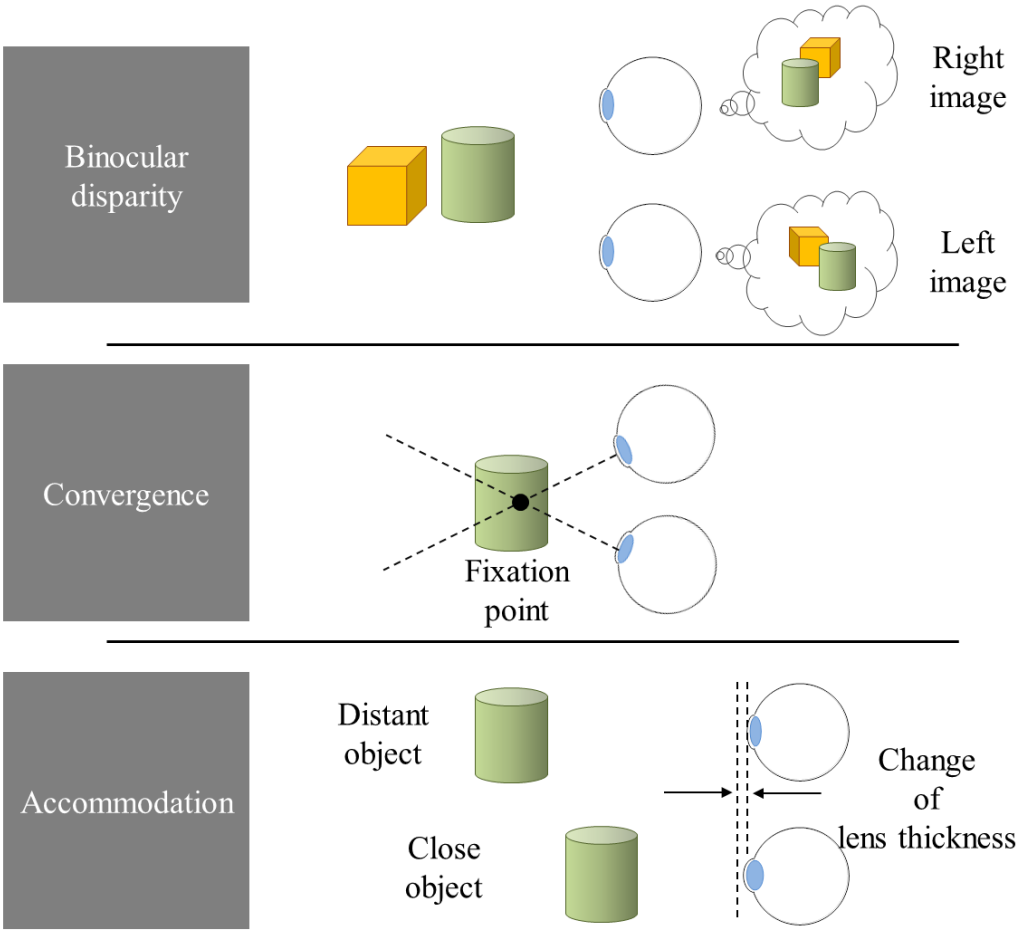
Binocular disparity
Right image
Left image
Convergence
Fixation point
Accommodation
Distant object
Close object
Change of lens thickness

(b)

Fig. 2.

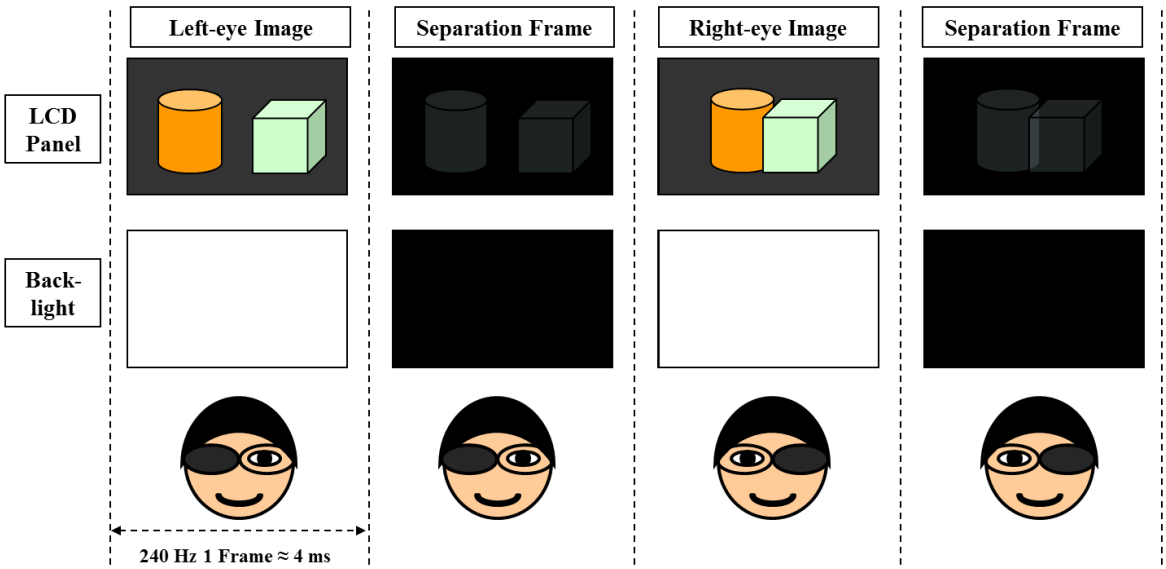
Left-eye Image
Separation Frame
Right-eye Image
Separation Frame
LCD Panel
Back-light
240 Hz 1 Frame ≈ 4 ms

Fig. 3.

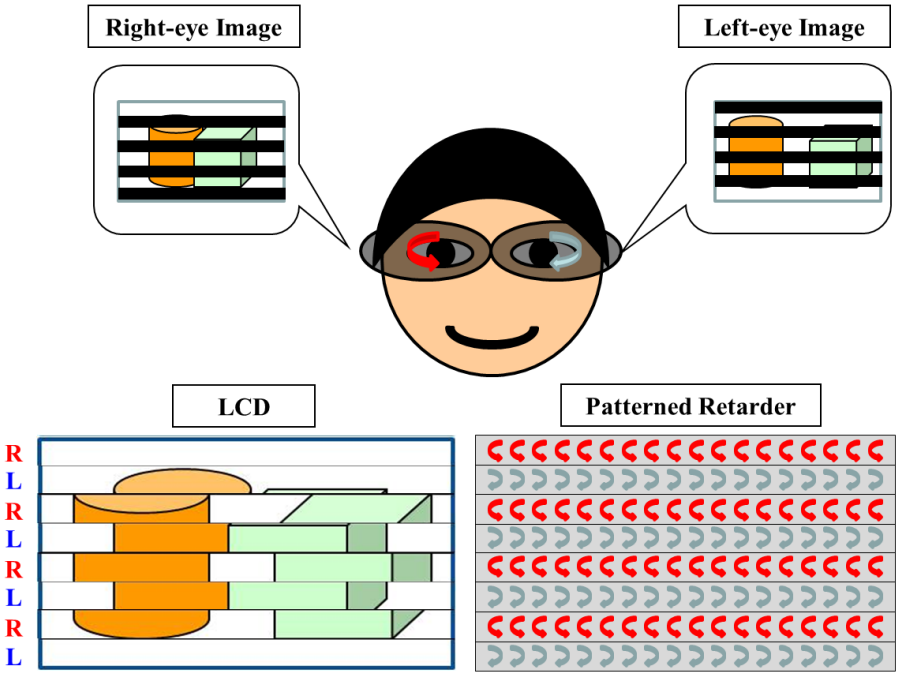
Right-eye Image
Left-eye Image
LCD
Patterned Retarder
R
L
R
L
R
L
R
L

Fig. 4.

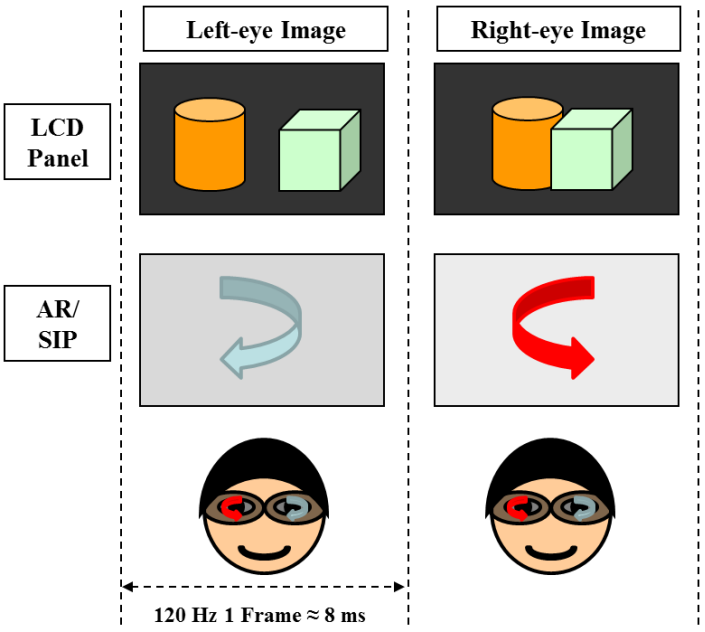
Left-eye Image
Right-eye Image
LCD Panel
AR/ SIP
120 Hz 1 Frame ≈ 8 ms

Fig. 5.

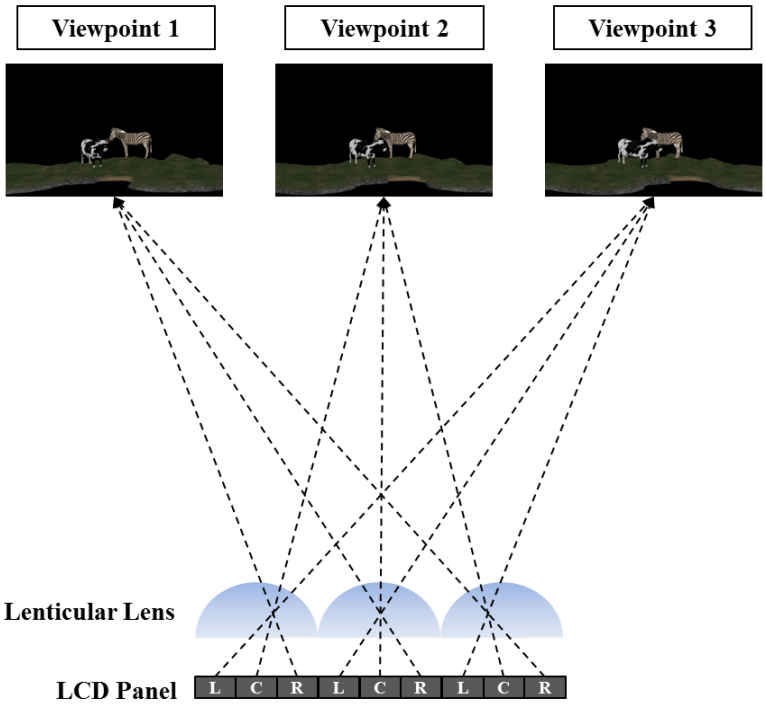
Viewpoint 1
Viewpoint 2
Viewpoint 3
Lenticular Lens
LCD Panel
L C R L C R L C R

Fig. 6.

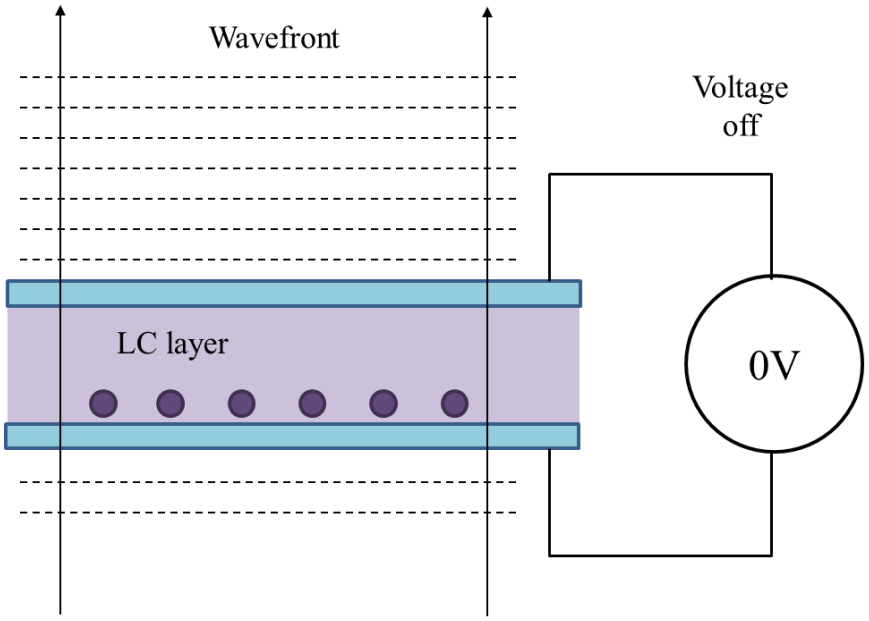
Wavefront
Voltage
off
LC layer
0V

(a)

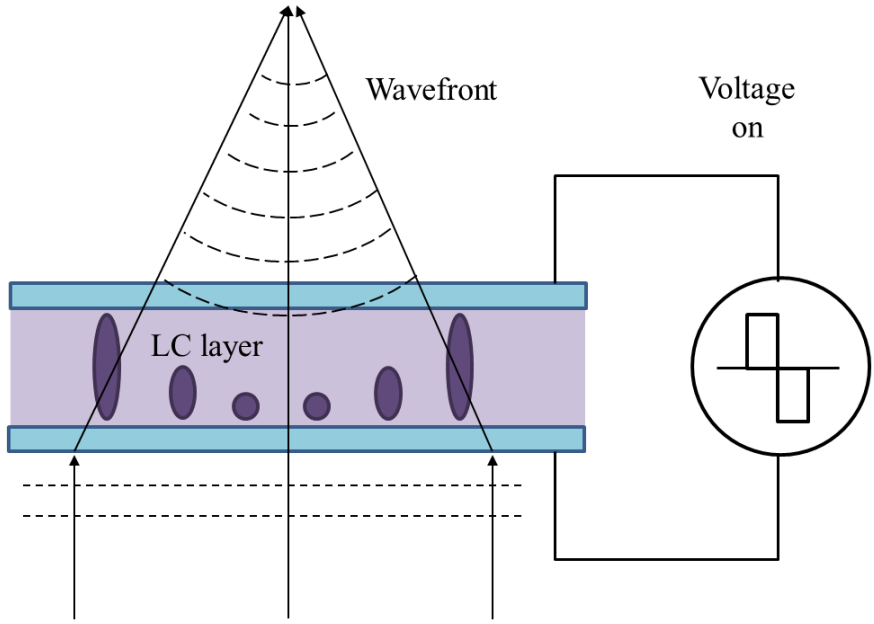
Wavefront
Voltage
on
LC layer

(b)

Fig. 7.

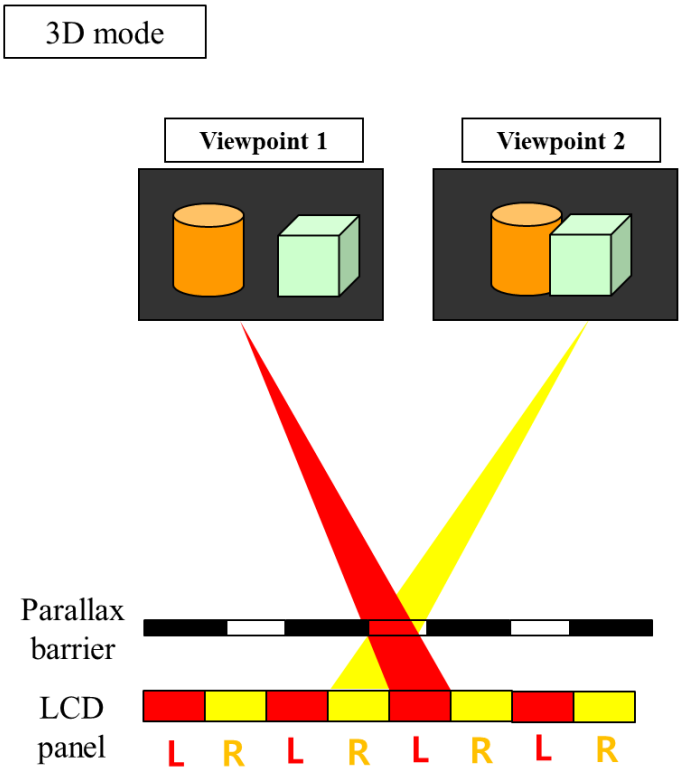
3D mode
Viewpoint 1
Viewpoint 2
Parallax barrier
LCD panel
L R L R L R L R

(a)

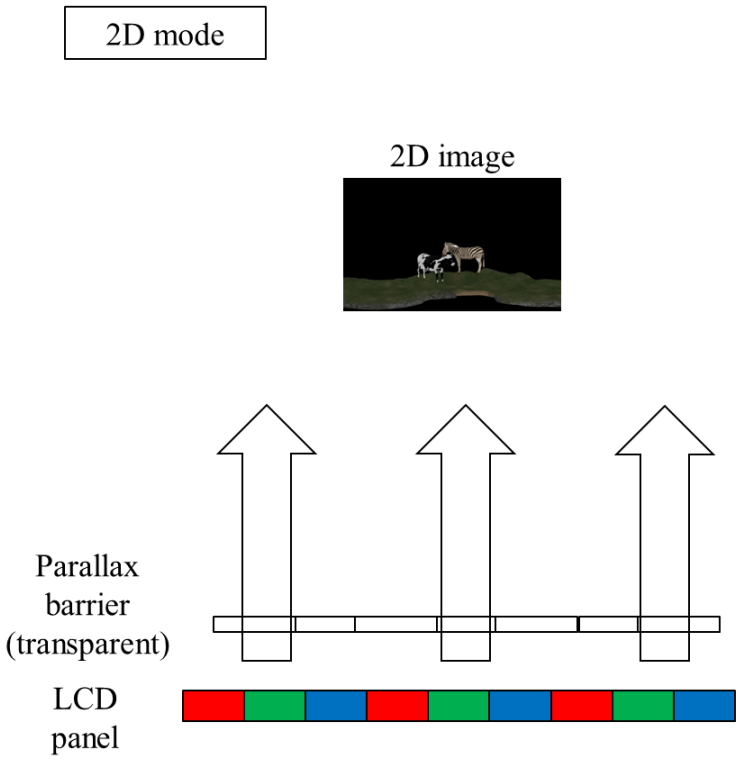

(b)

Fig. 8.

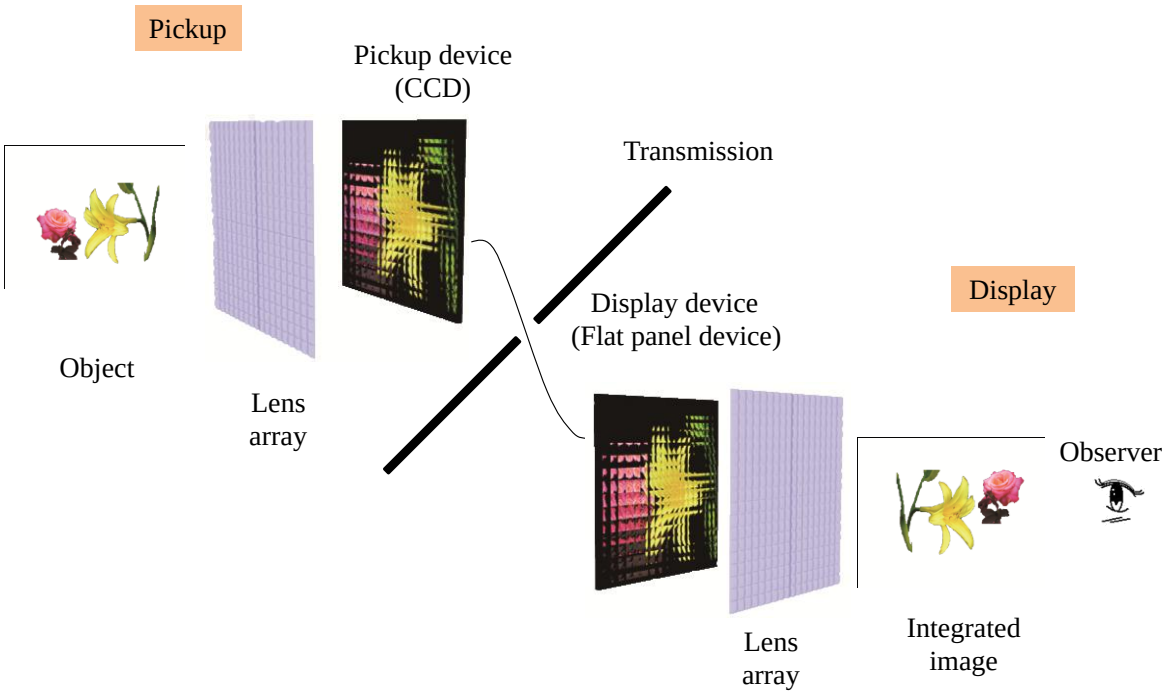
Pickup
Pickup device
(CCD)
Transmission
Display
Display device
(Flat panel device)
Object
Lens
array
Lens
array
Observer
Integrated
image

Fig. 9.

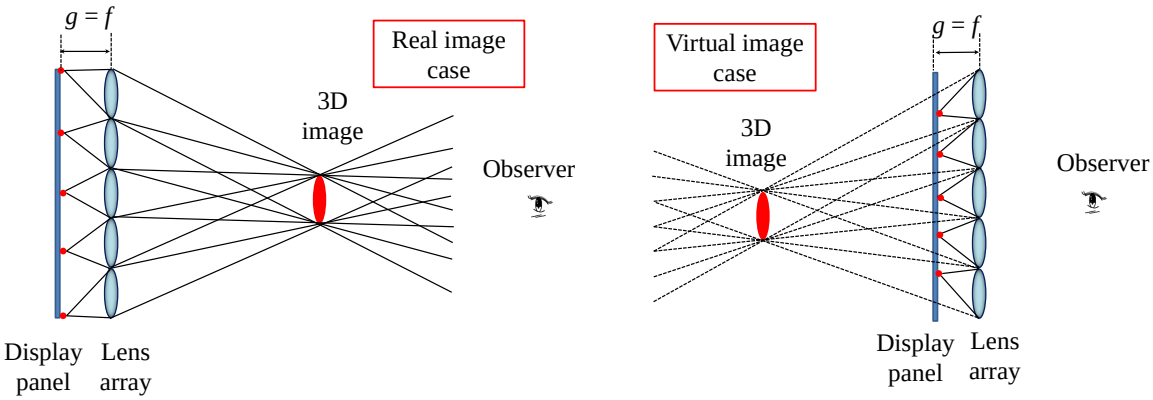
g = f
Real image case
3D image
Observer
Display panel
Lens array
Virtual image case
g = f
3D image
Observer
Display panel
Lens array

(a)

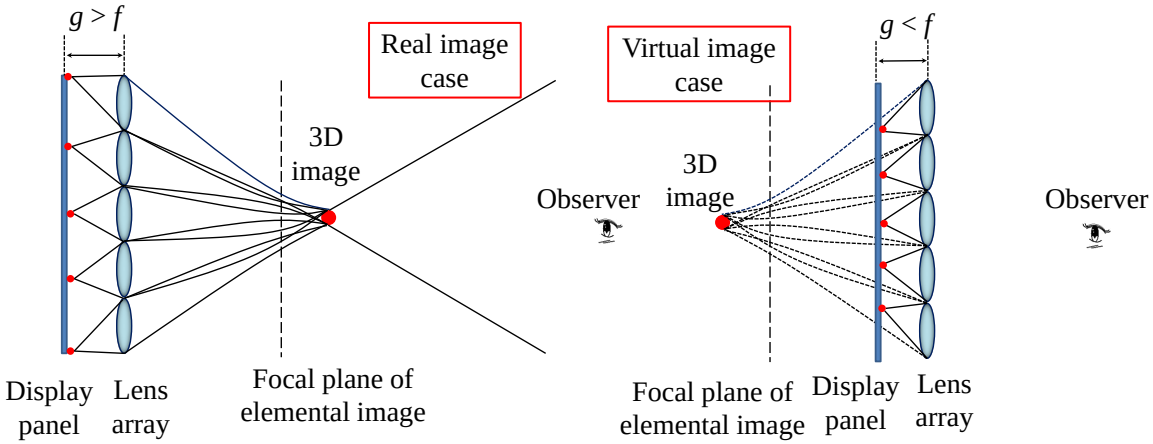
g > f
Real image case
3D image
Display panel
Lens array
Focal plane of elemental image
Virtual image case
g < f
Observer
3D image
Observer
Focal plane of elemental image
Display panel
Lens array

(b)

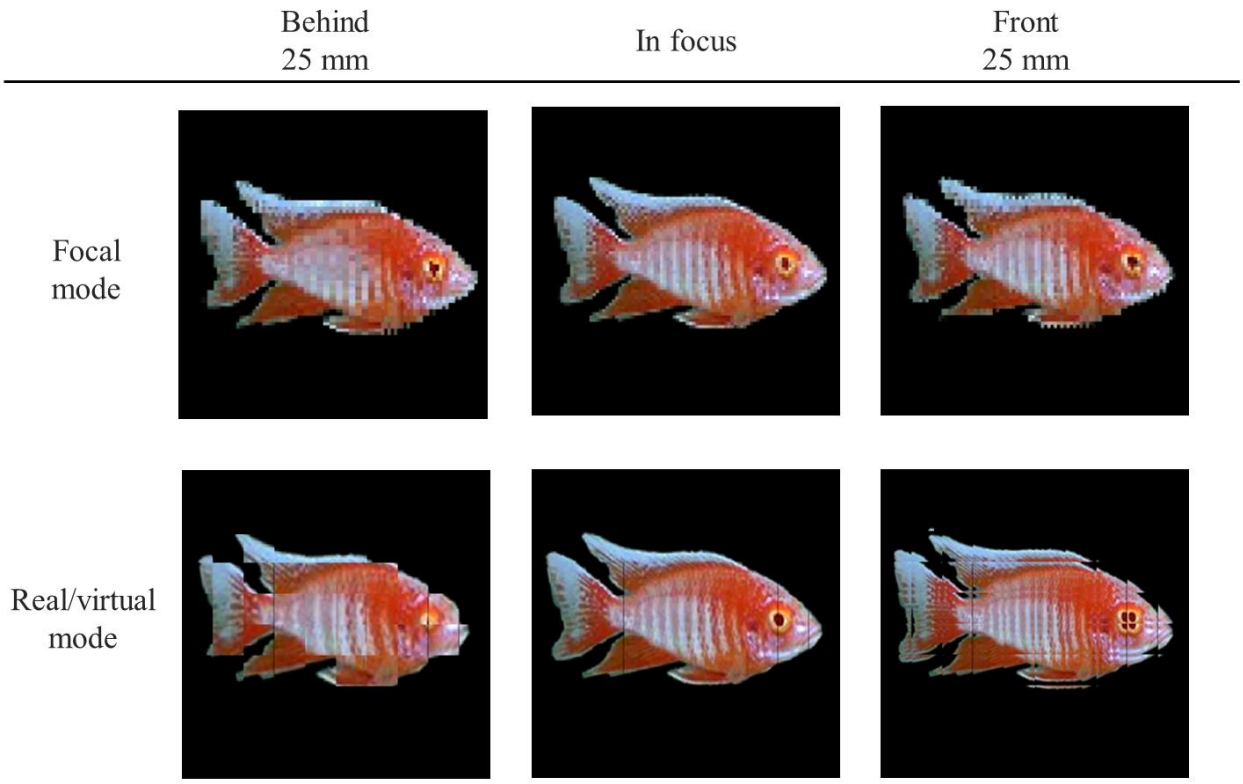
Behind
25 mm
In focus
Front
25 mm
Focal
mode
Real/virtual
mode

(c)

Fig. 10.

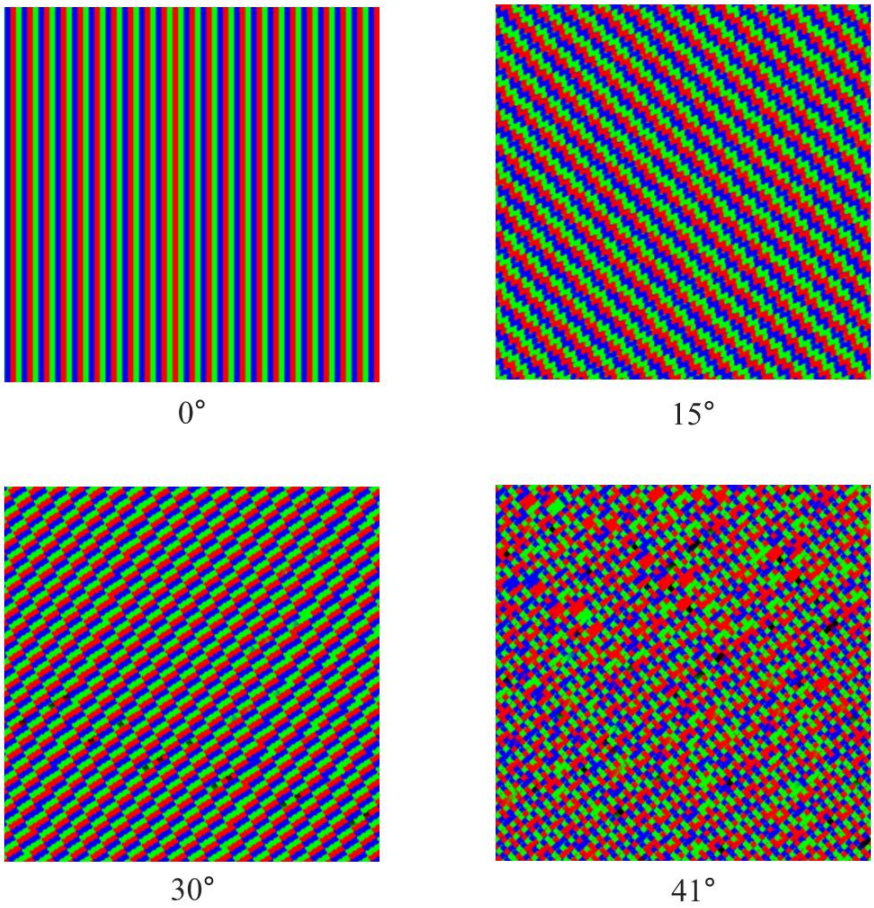

Fig. 11.

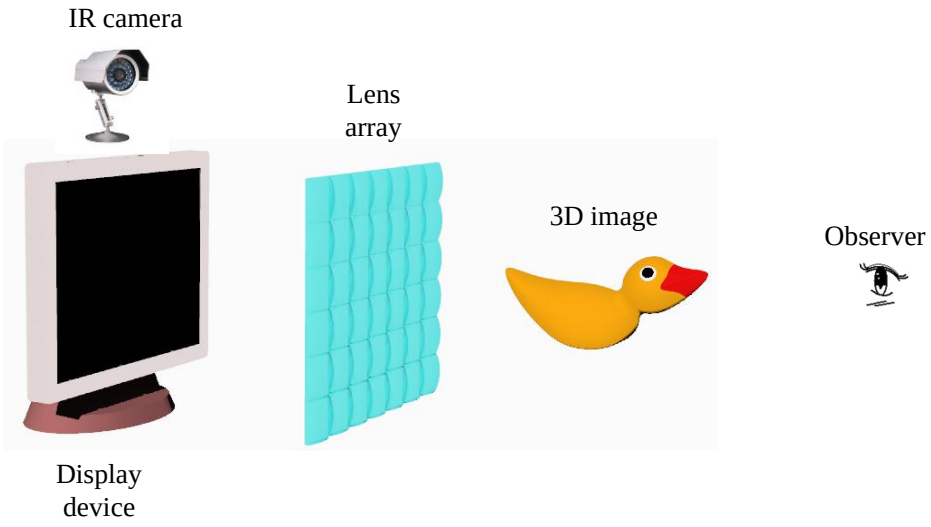
IR camera
Lens
array
3D image
Observer
Display
device

(a)

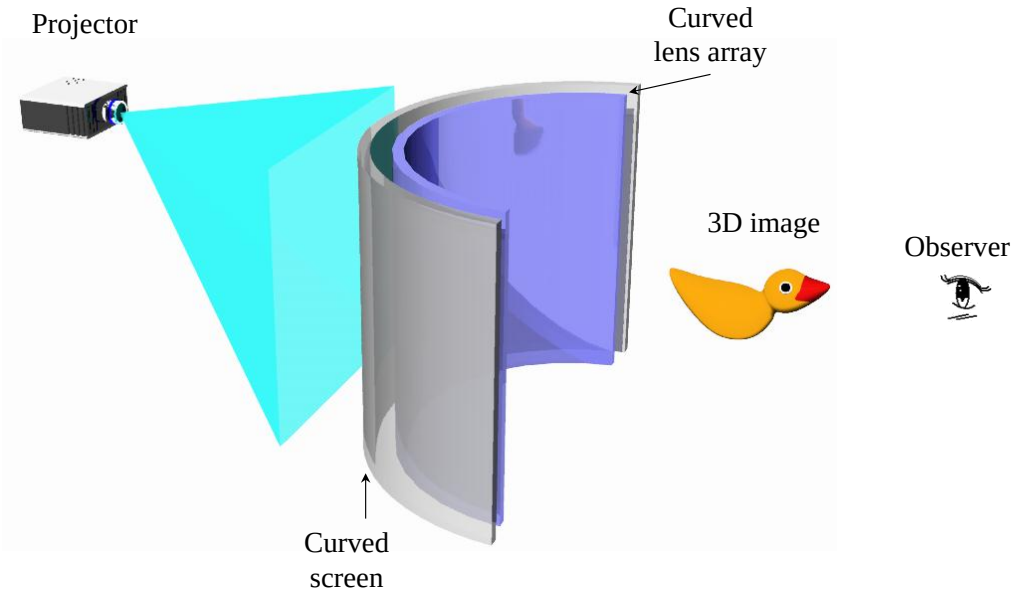
Projector
Curved
lens array
3D image
Observer
Curved
screen

(b)

Fig. 12.

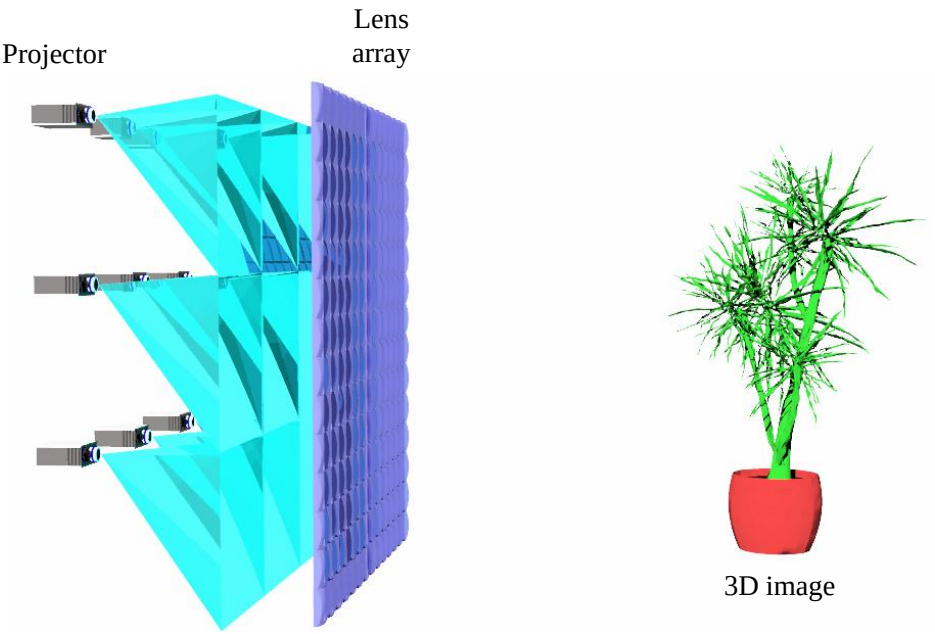

Fig. 13.

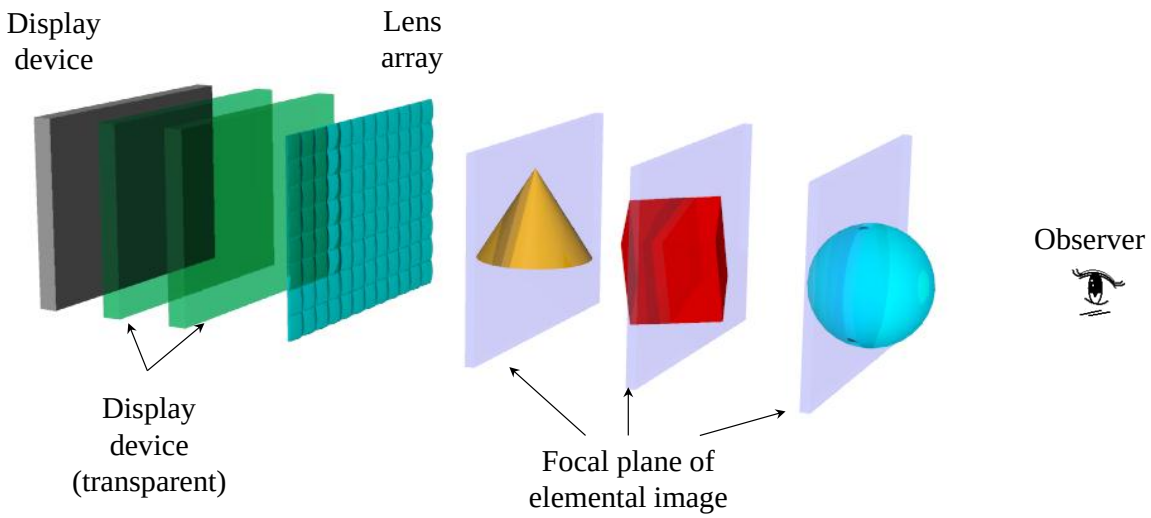
Display device
Lens array
Observer
Display device (transparent)
Focal plane of elemental image

(a)

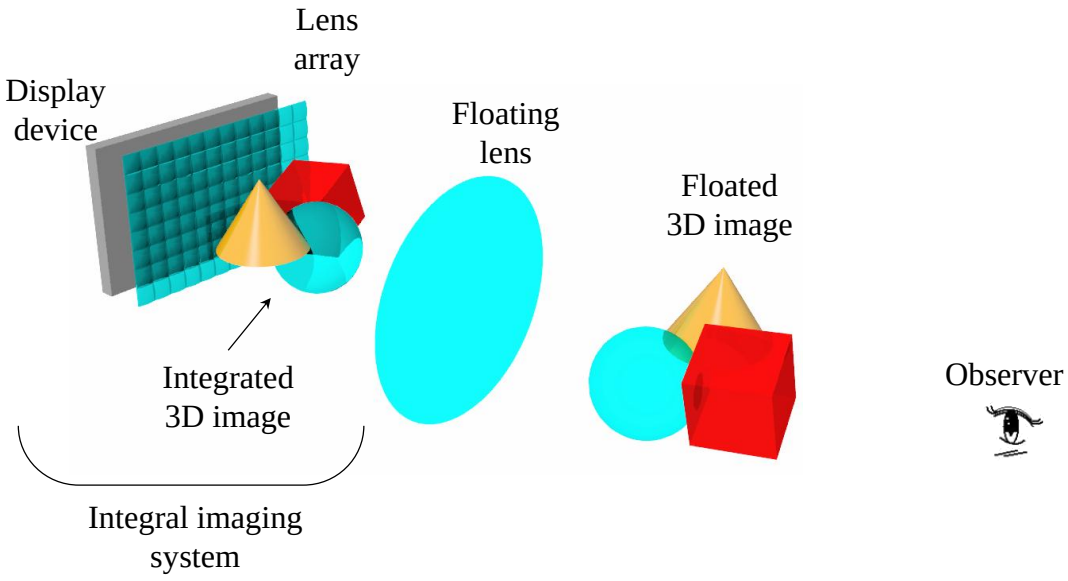
Lens array
Display device
Floating lens
Floated 3D image
Observer
Integrated 3D image
Integral imaging system

(b)

Fig. 14.

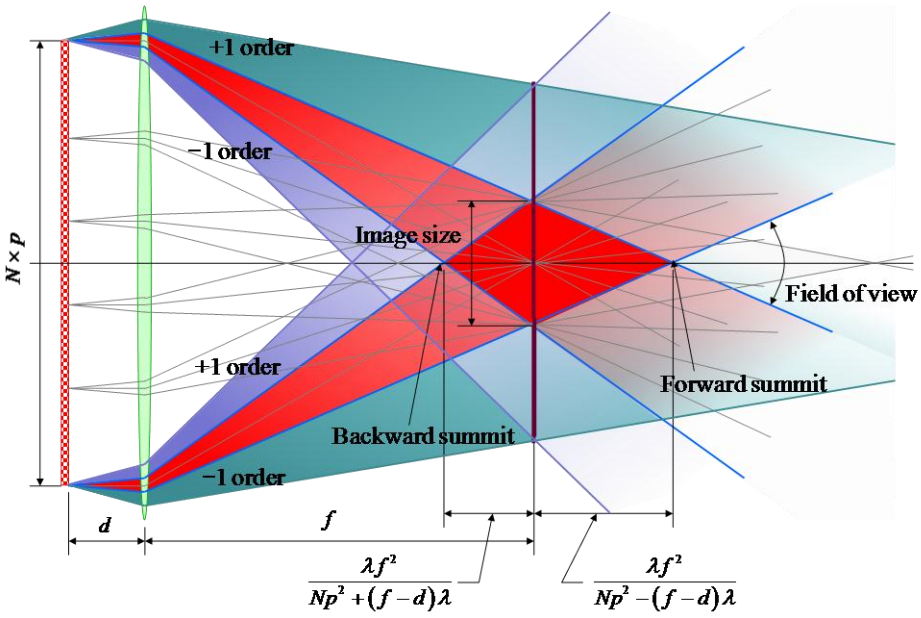
+1 order
−1 order
Image size
N × p
Field of view
+1 order
Forward summit
Backward summit
−1 order
d
f
$\frac{\lambda f^2}{Np^2+(f-d)\lambda}$
$\frac{\lambda f^2}{Np^2-(f-d)\lambda}$

(a)

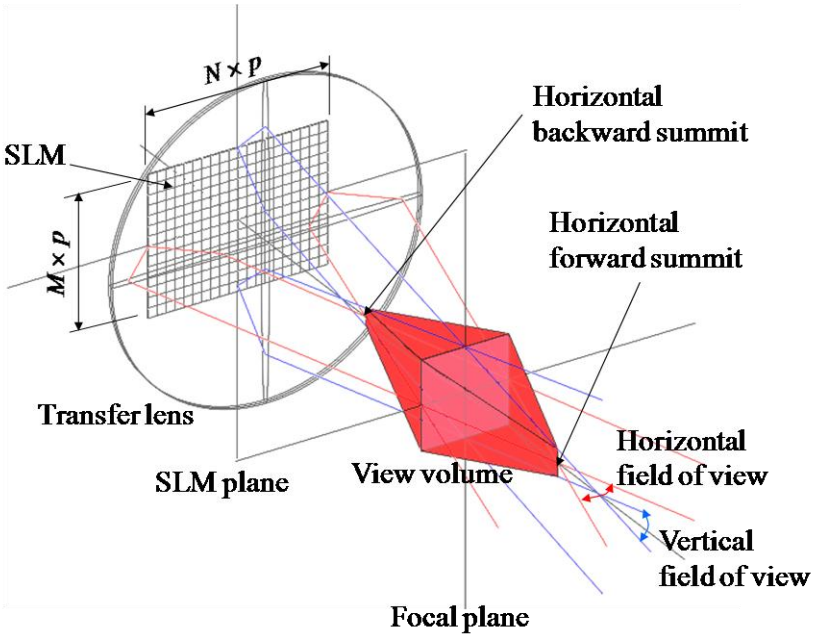
N × p
Horizontal
backward summit
SLM
Horizontal
forward summit
M × p
Transfer lens
SLM plane
View volume
Horizontal
field of view
Vertical
field of view
Focal plane

(b)

Fig. 15.

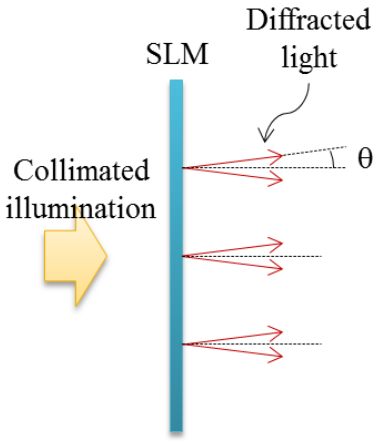
Diffracted
light
SLM
θ
Collimated
illumination

(a)

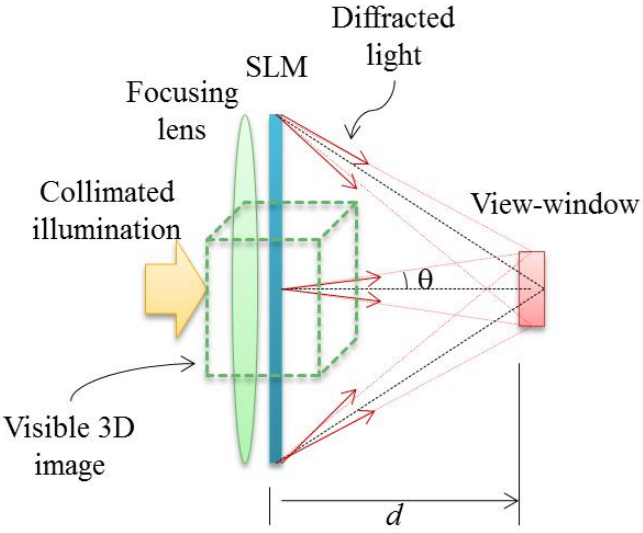
Diffracted
light
SLM
Focusing
lens
Collimated
illumination
View-window
θ
Visible 3D
image
d

(b)

Fig. 16.

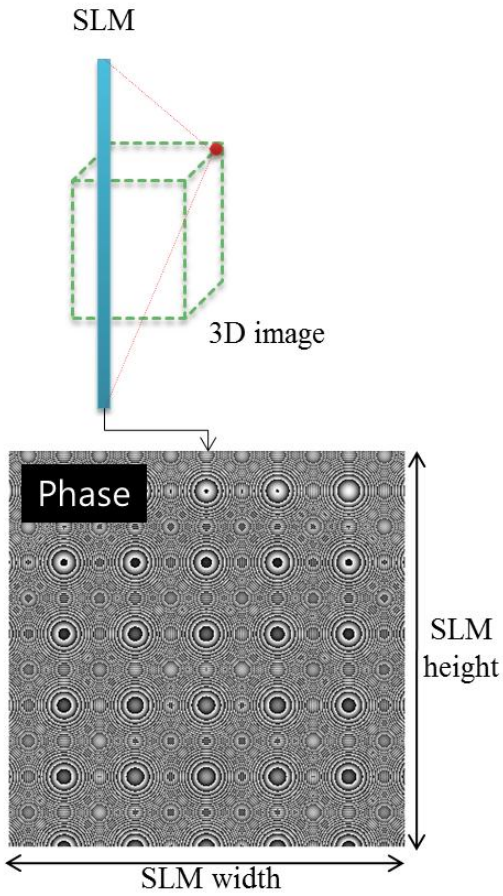

(a)

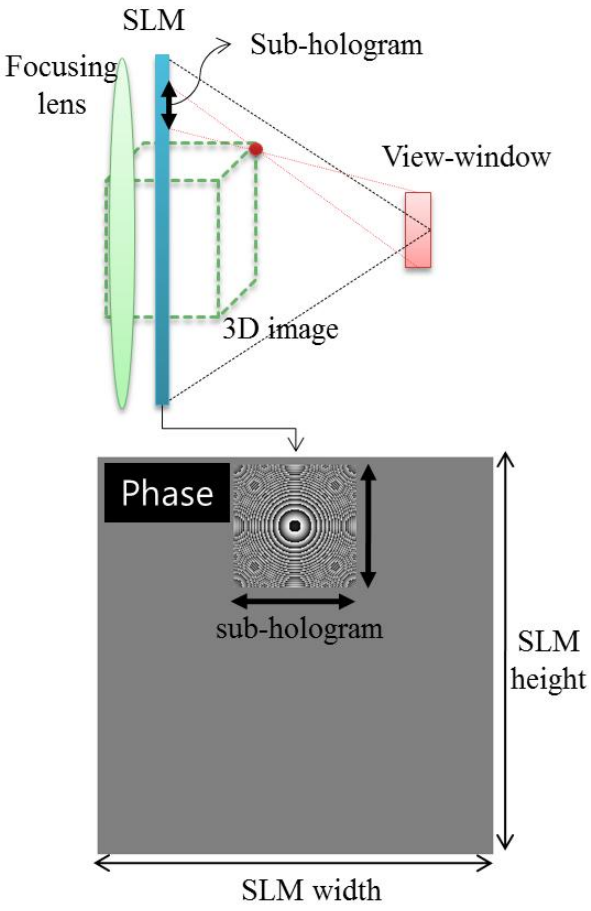
SLM
Sub-hologram
Focusing lens
View-window
3D image
Phase
sub-hologram
SLM height
SLM width

(b)

Fig. 17.

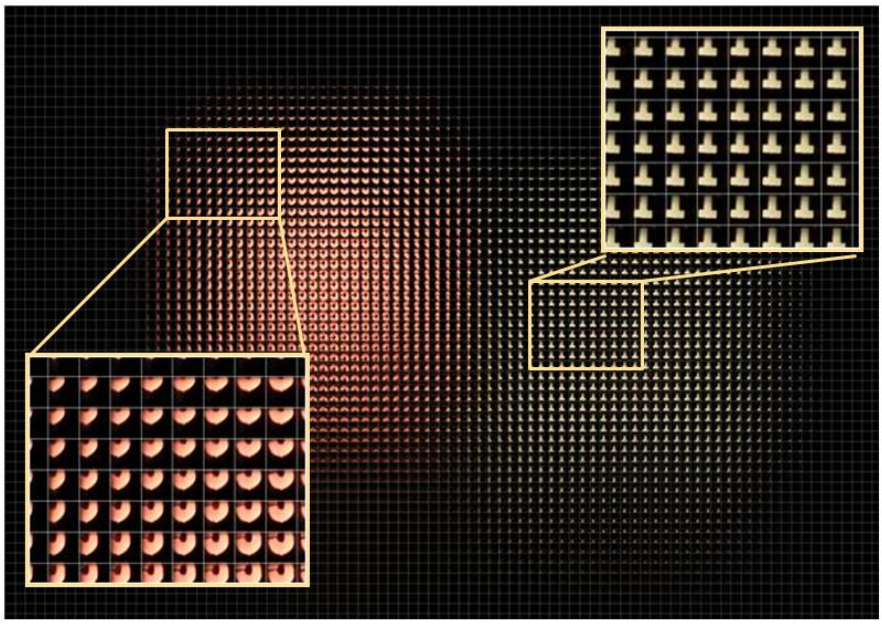

(a)

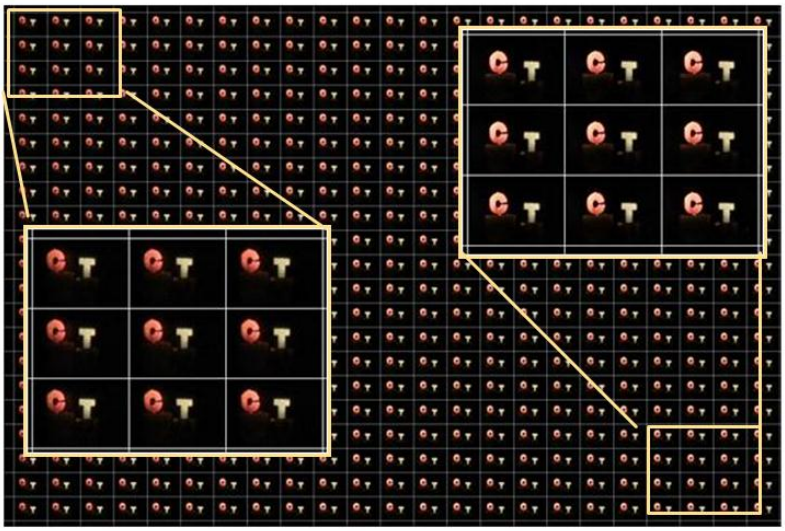

(b)

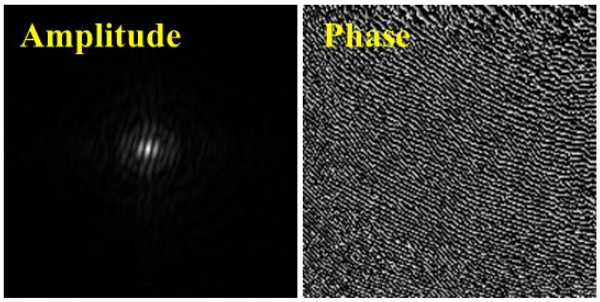

(c)

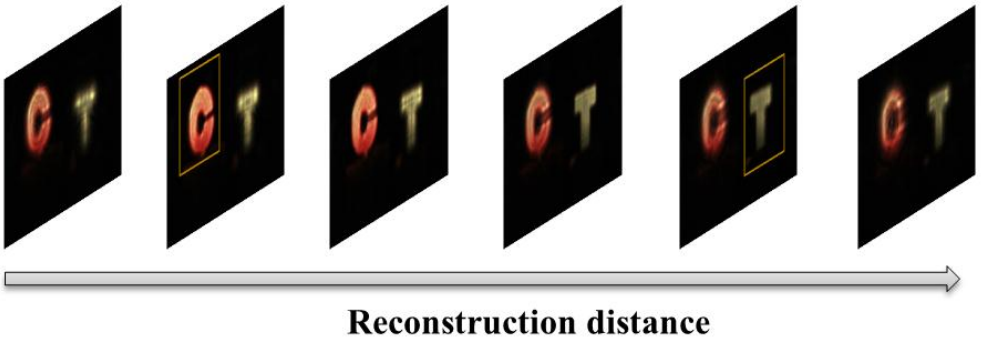

(d)

Fig. 18.

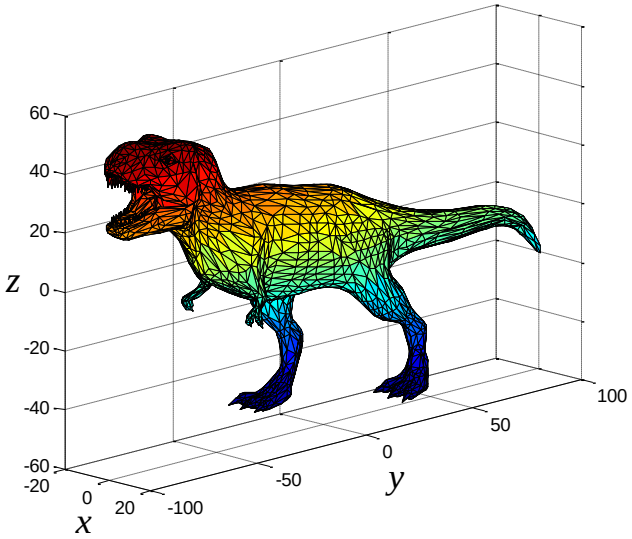

Fig. 19.

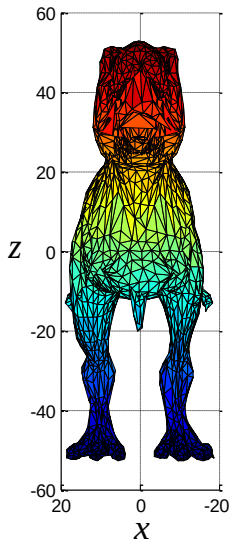
60
40
20
z 0
-20
-40
-60
20
0
-20
x

(a)

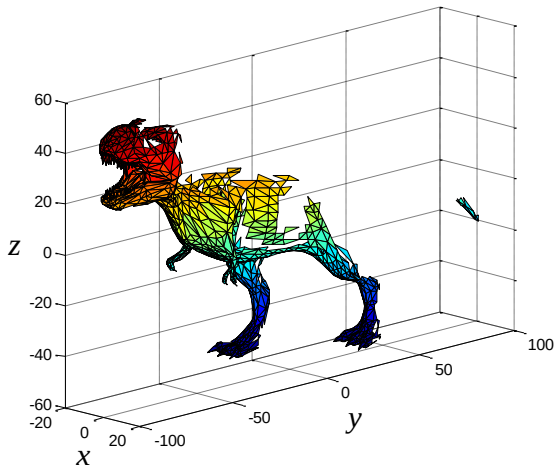
60
40
20
z 0
-20
-40
-60
-20
0
20
x
-100
-50
0
50
100
y

(b)

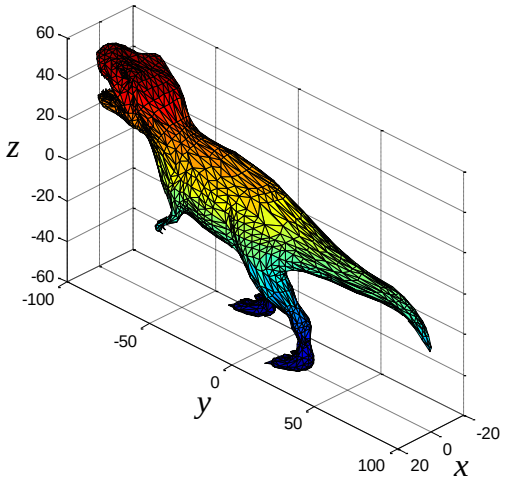
60
40
20
z
0
-20
-40
-60
-100
-50
0
y
50
100
-20
0
20
x

(c)

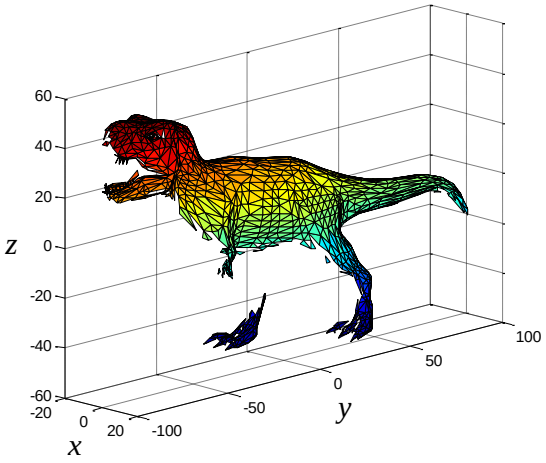
60
40
20
z
0
-20
-40
-60
-20
0
20
x
-100
-50
0
y
50
100

(d)

Fig. 20.

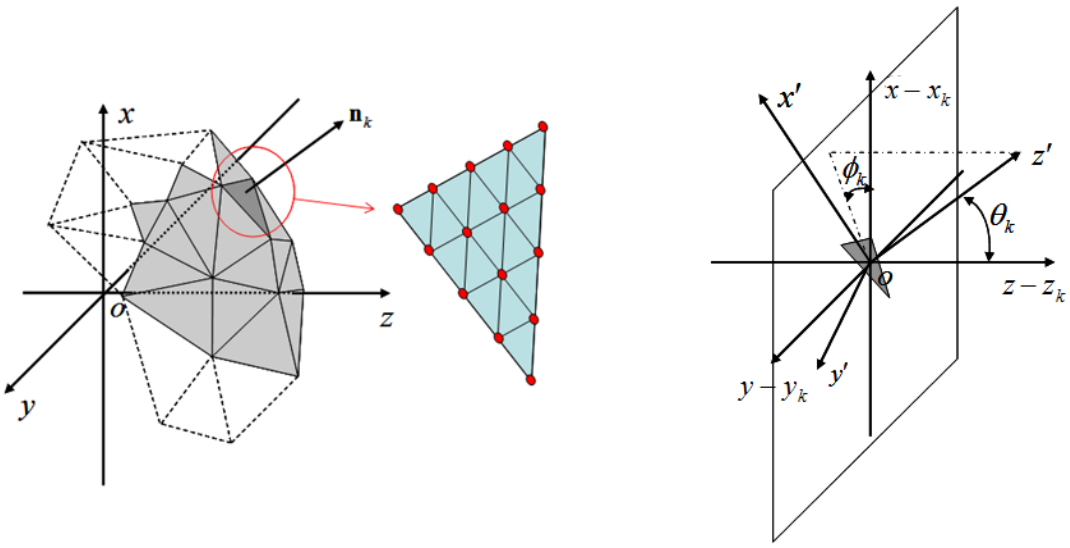

Fig. 21.

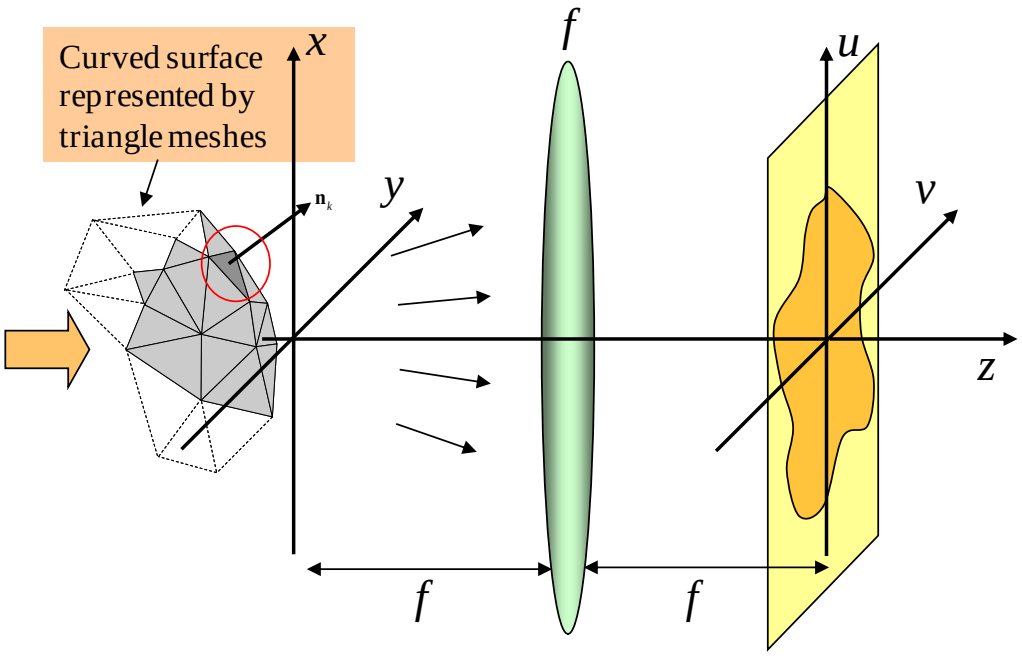
Curved surface
represented by
triangle meshes
x
y
z
f
f
u
v
f

(a)

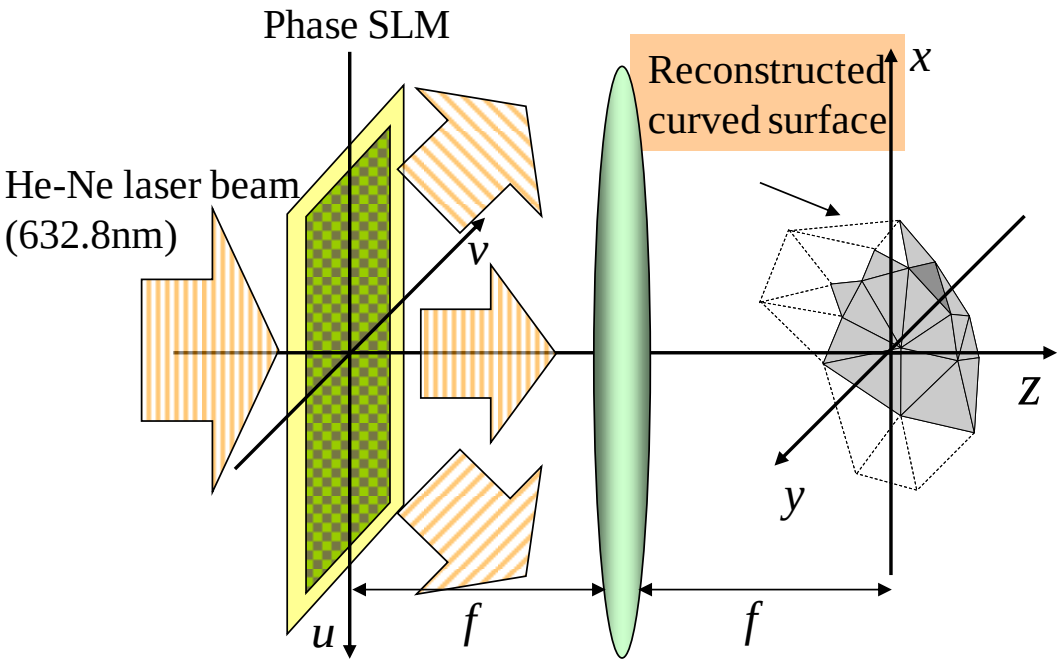
Phase SLM
He-Ne laser beam
(632.8nm)
Reconstructed
curved surface
x
y
z
u
v
f
f

(b)

Fig. 22.

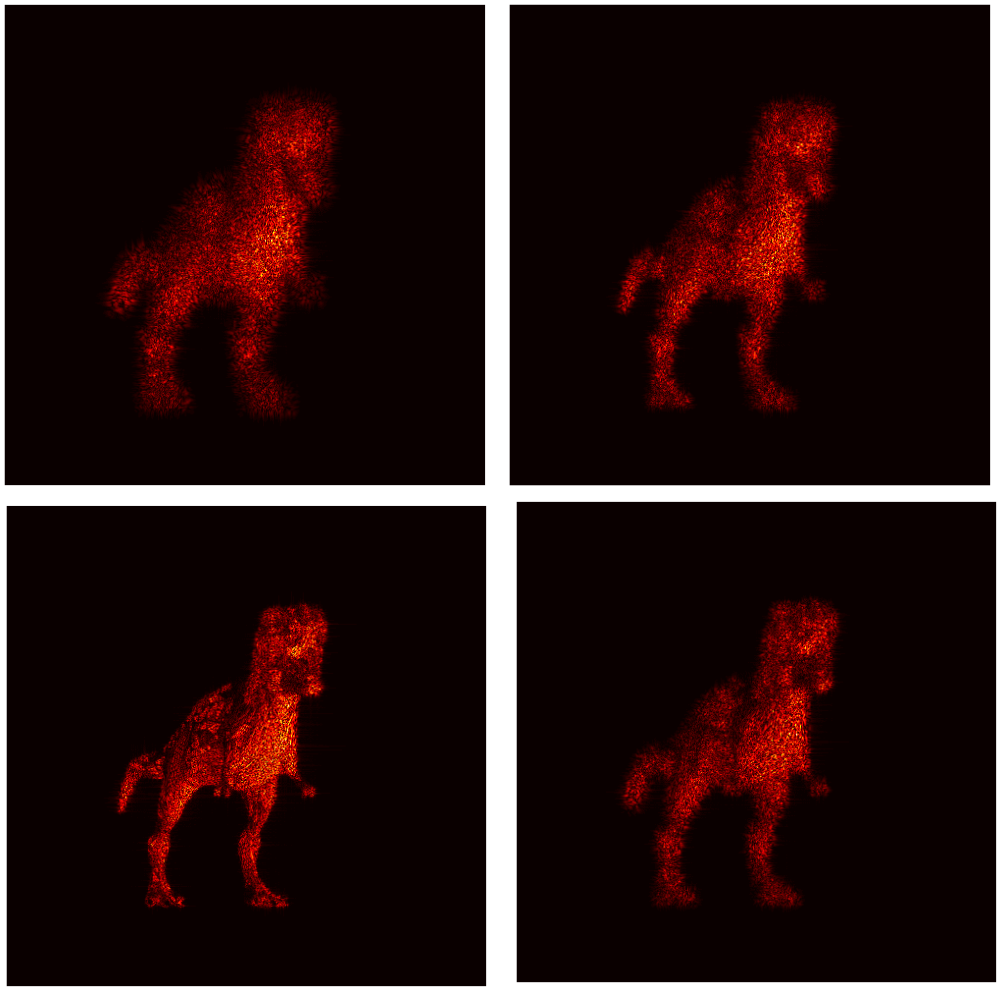

Fig. 23.

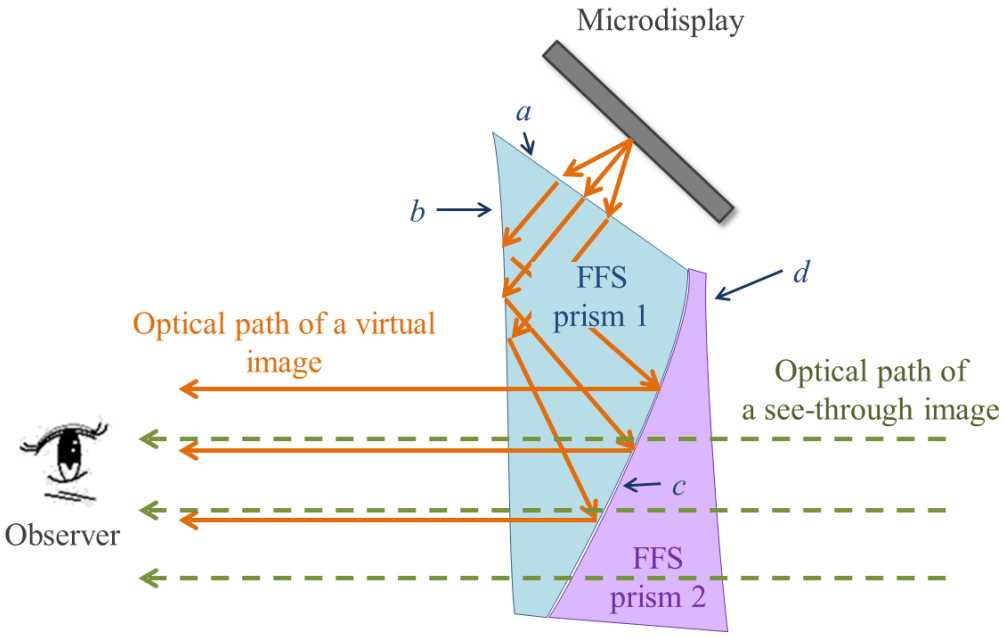
Microdisplay
a
b
d
FFS
prism 1
Optical path of a virtual
image
Optical path of
a see-through image
c
Observer
FFS
prism 2

Fig. 24.

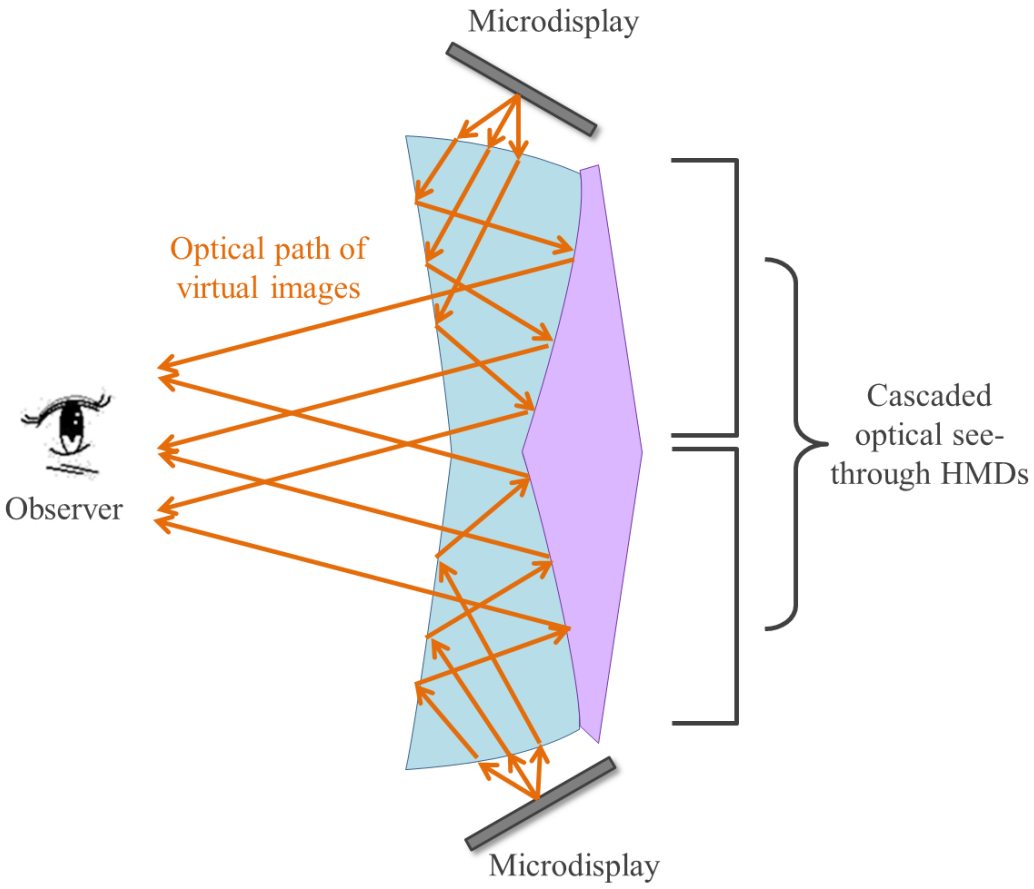
Microdisplay
Optical path of
virtual images
Observer
Cascaded
optical see-
through HMDs
Microdisplay

Fig. 25.

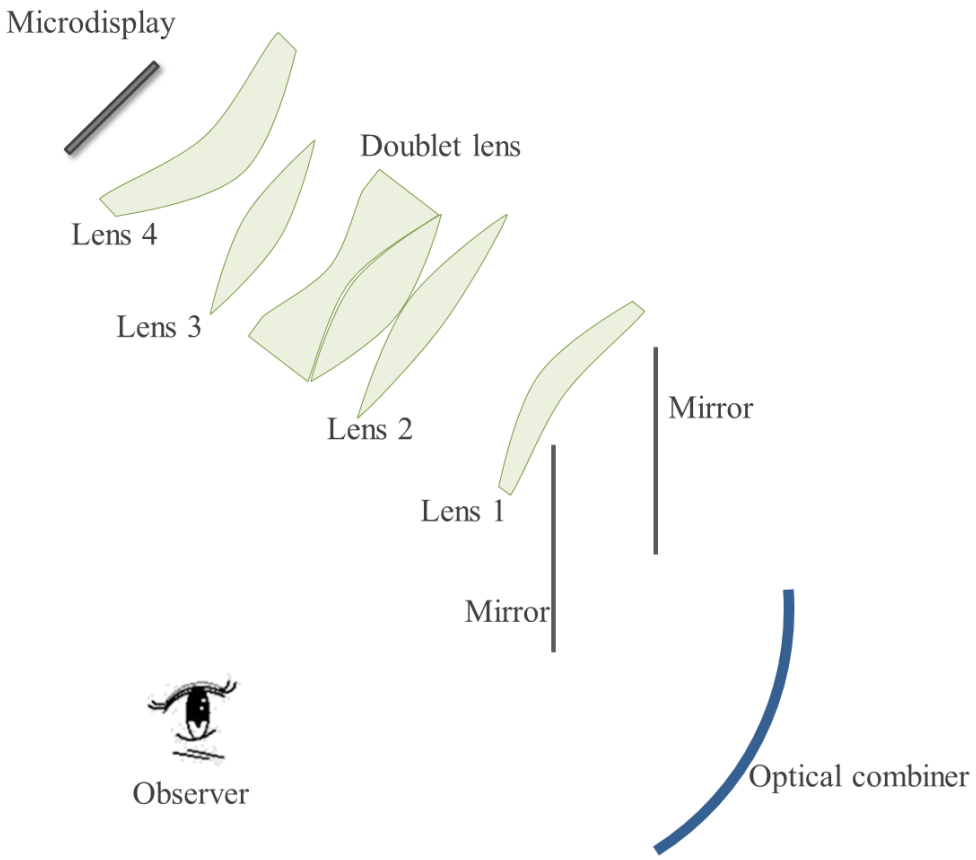
Microdisplay
Doublet lens
Lens 4
Lens 3
Lens 2
Lens 1
Mirror
Mirror
Observer
Optical combiner

Fig. 26.

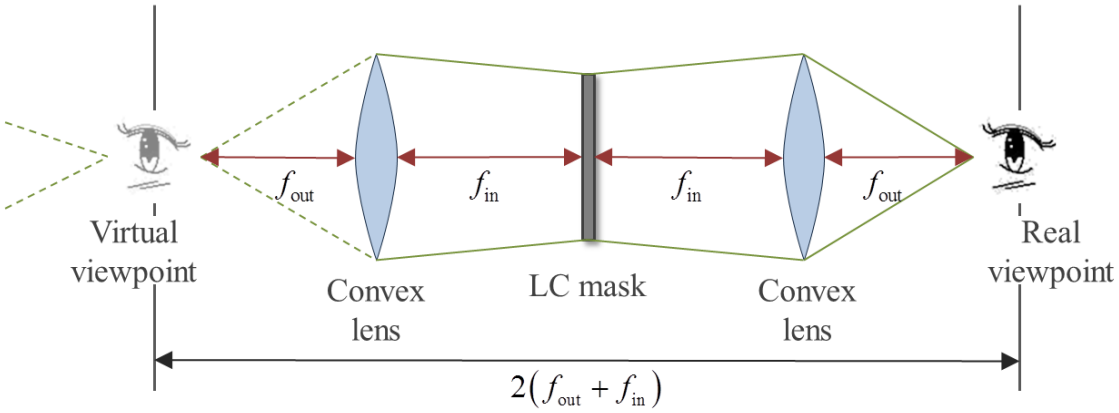
f_{out}
f_{in}
f_{in}
f_{out}
Virtual viewpoint
Convex lens
LC mask
Convex lens
Real viewpoint
$2(f_{out} + f_{in})$

(a)

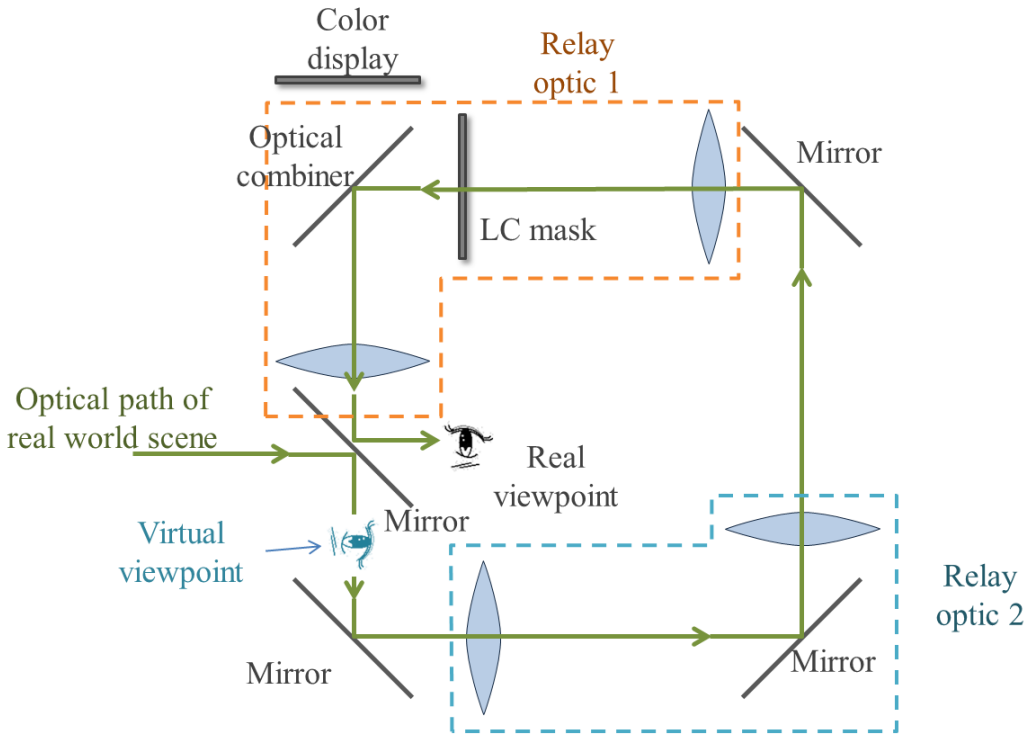
Color display
Relay optic 1
Optical combiner
Mirror
LC mask
Optical path of real world scene
Real viewpoint
Virtual viewpoint
Mirror
Relay optic 2
Mirror
Mirror

(b)

Fig. 27.

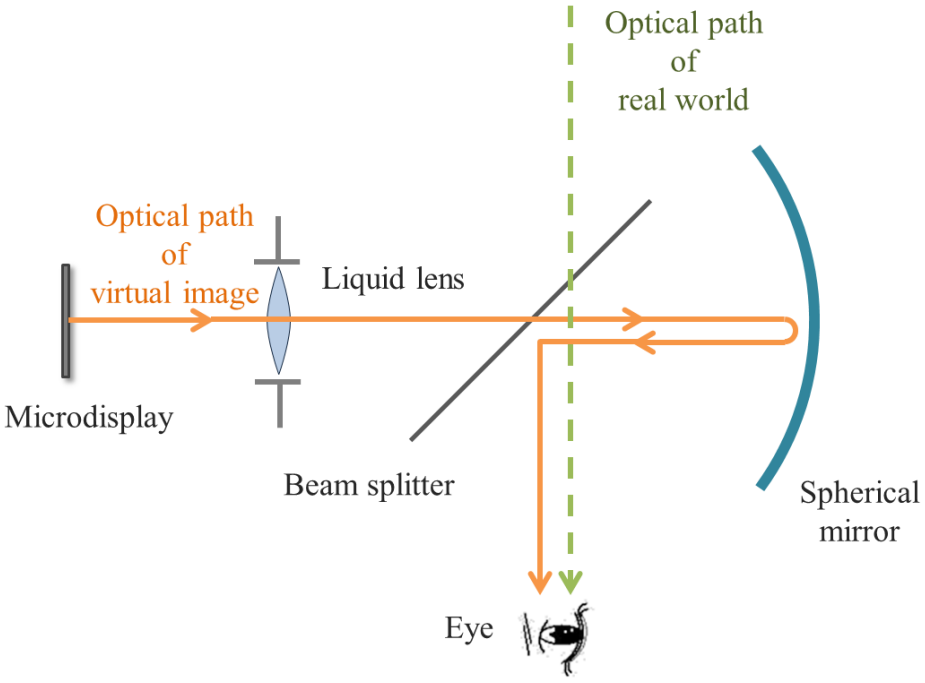
Optical path
of
real world
Optical path
of
virtual image
Liquid lens
Microdisplay
Beam splitter
Spherical
mirror
Eye

Fig. 28.

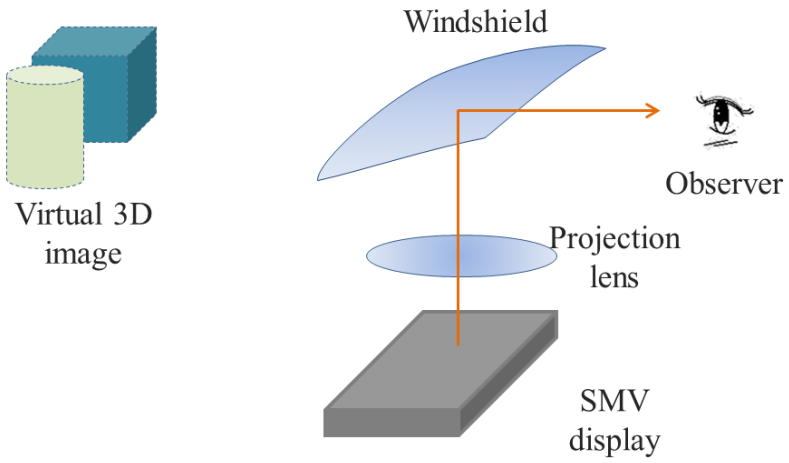
Windshield
Observer
Virtual 3D
image
Projection
lens
SMV
display

(a)

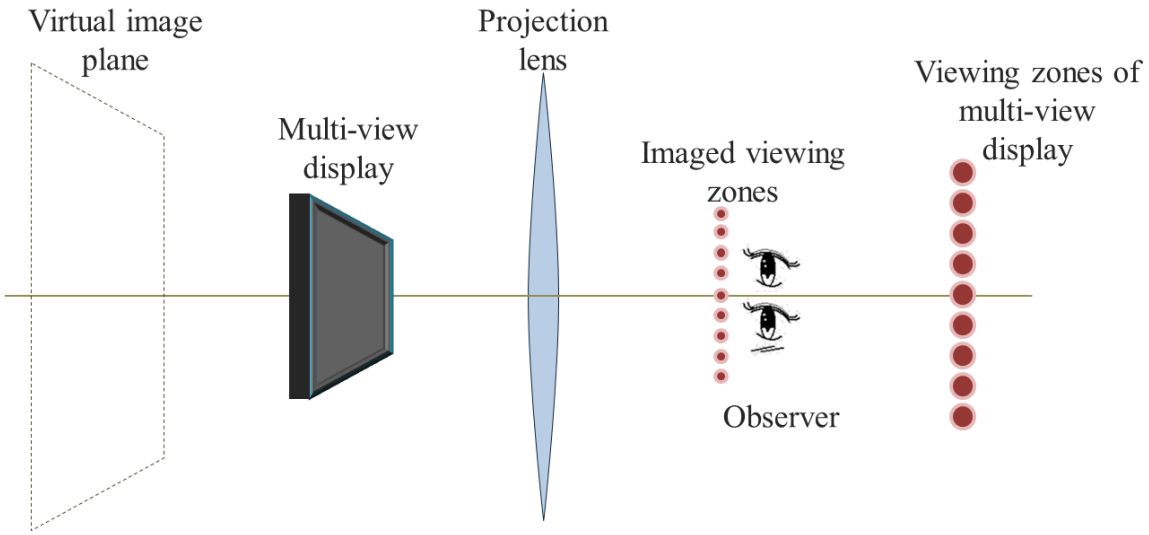
Virtual image
plane
Multi-view
display
Projection
lens
Imaged viewing
zones
Viewing zones of
multi-view
display
Observer

(b)

Fig. 29.

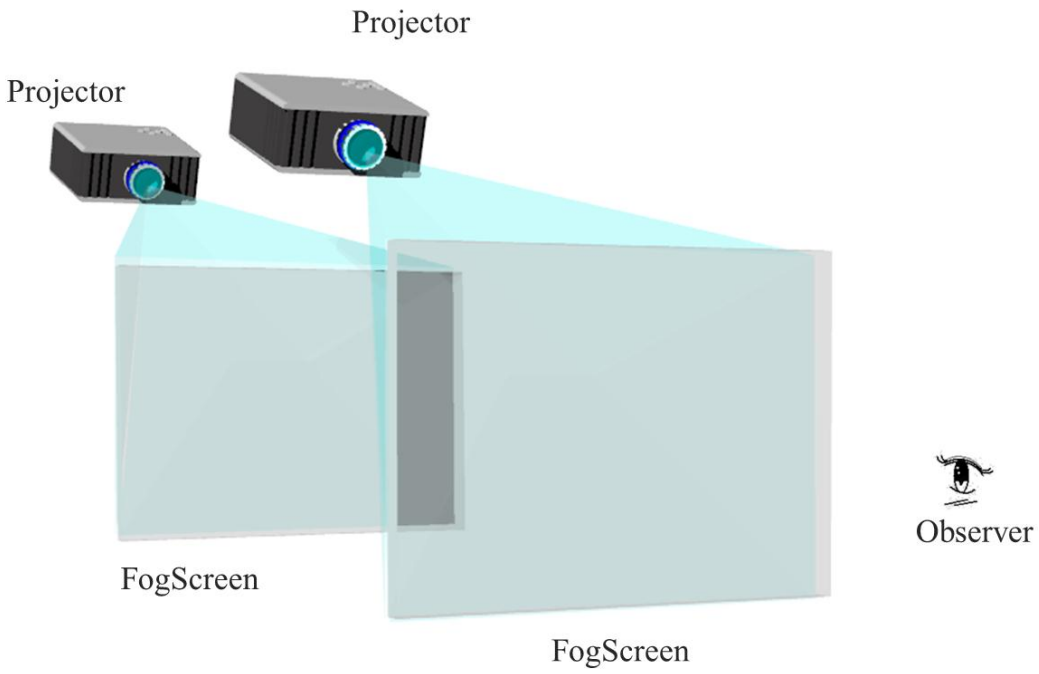

Fig. 30.

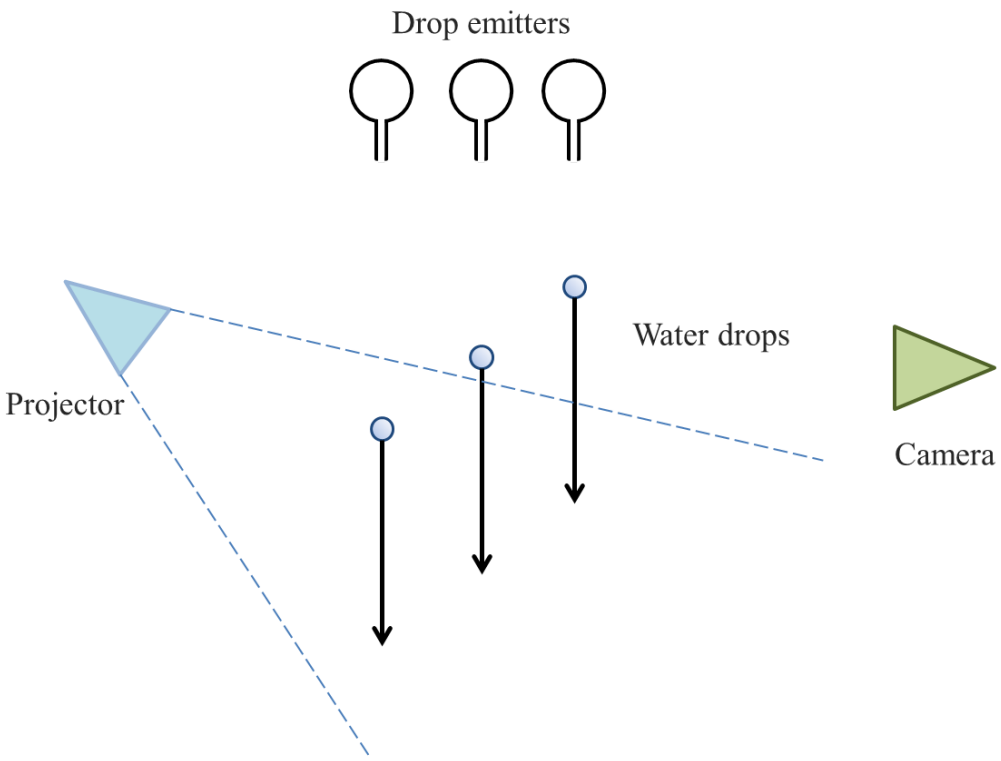
Drop emitters
Water drops
Projector
Camera

(a)

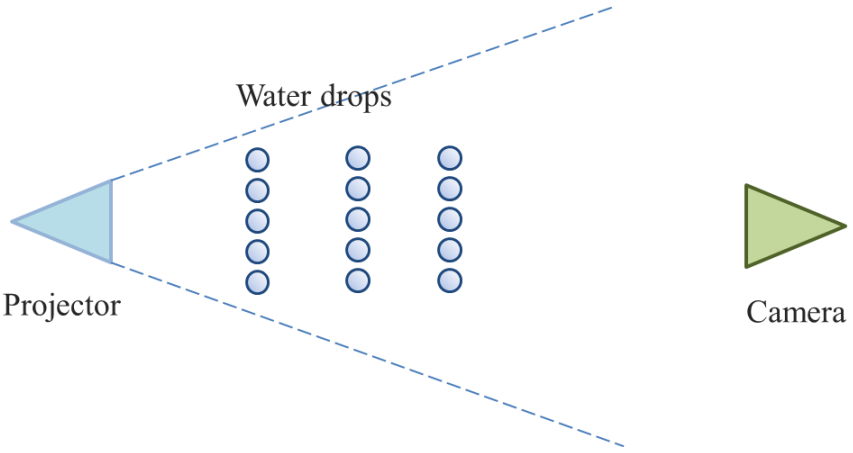
Water drops
Projector
Camera

(b)

Fig. 31.

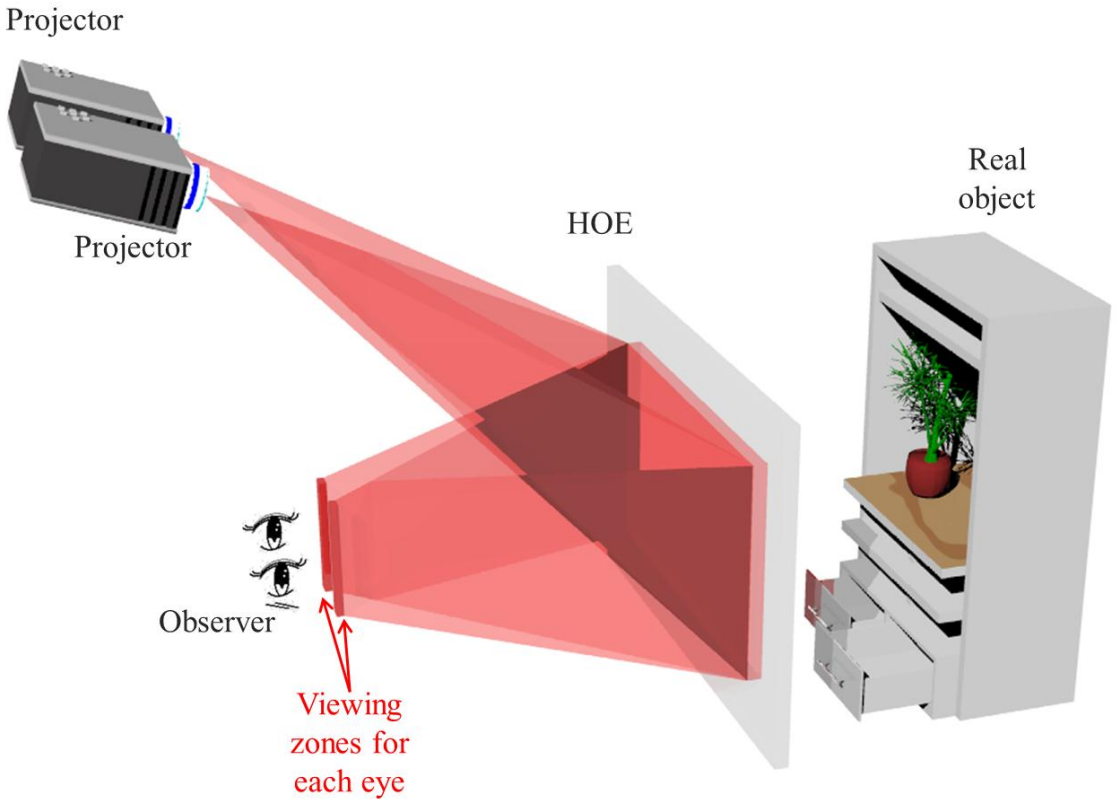
Projector
Projector
HOE
Real
object
Observer
Viewing
zones for
each eye

Fig. 32.

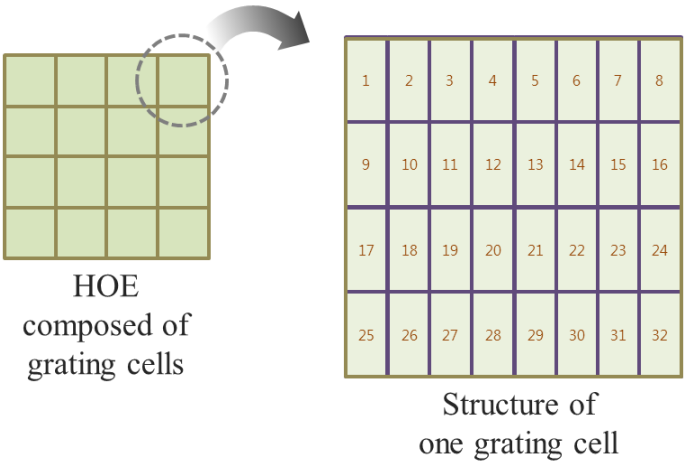
1 2 3 4 5 6 7 8
9 10 11 12 13 14 15 16
17 18 19 20 21 22 23 24
25 26 27 28 29 30 31 32
HOE
composed of
grating cells
Structure of
one grating cell

(a)

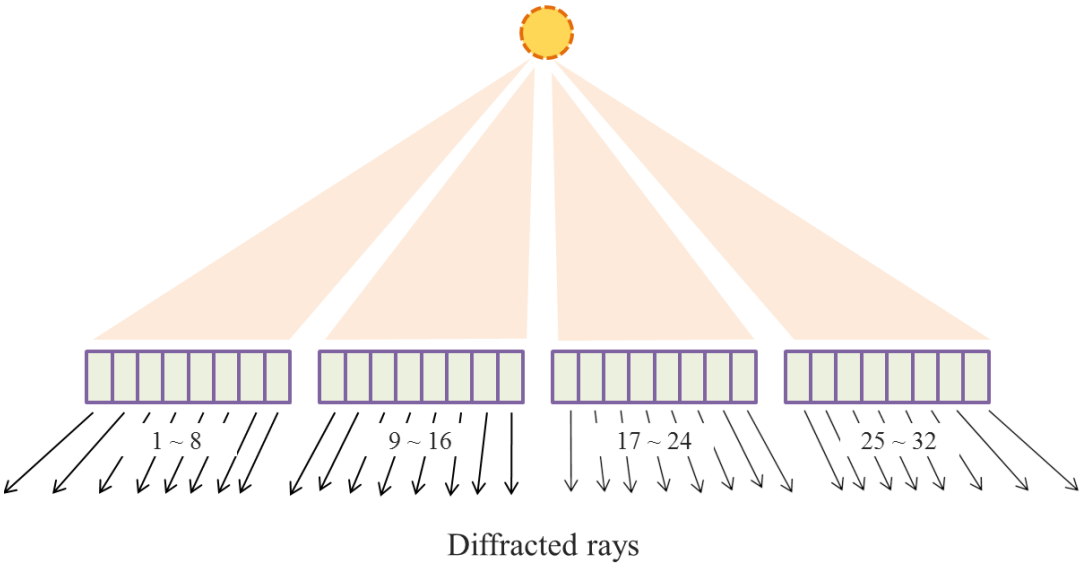
1 ~ 8
9 ~ 16
17 ~ 24
25 ~ 32
Diffracted rays

(b)

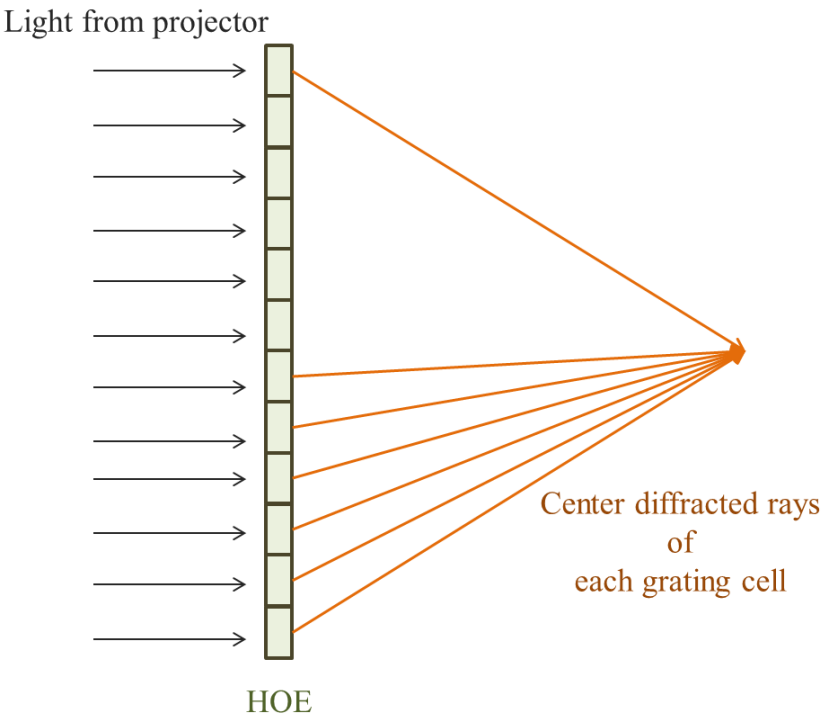
Light from projector
Center diffracted rays
of
each grating cell
HOE

(c)

Fig. 33.

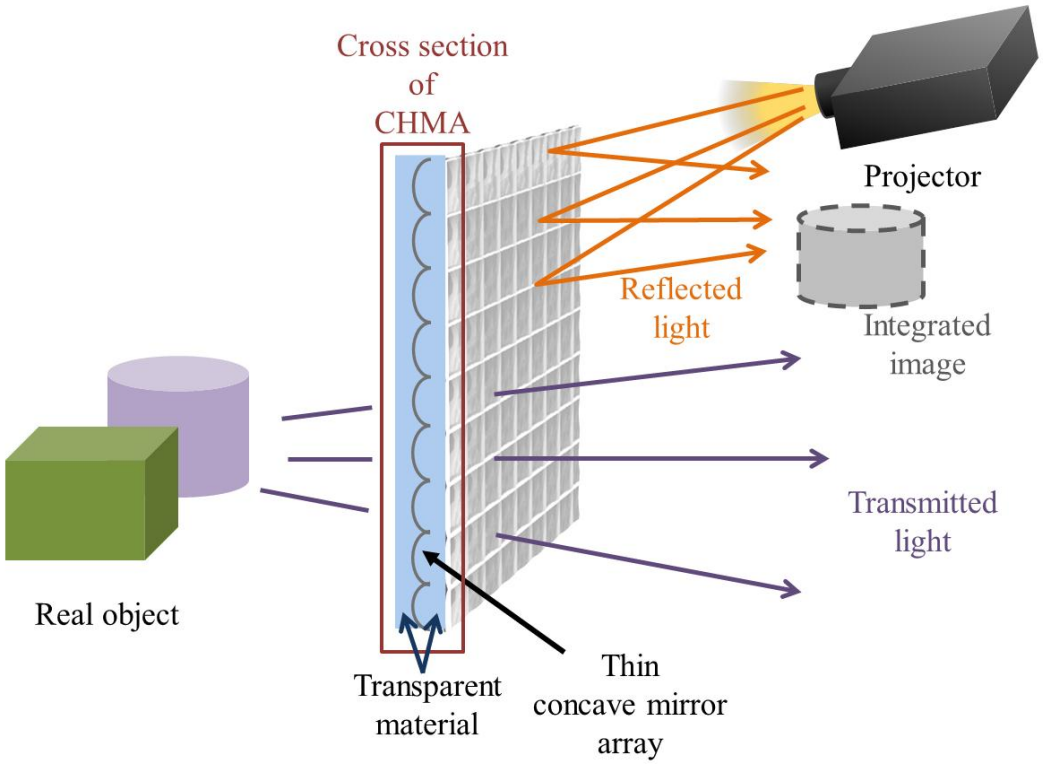
Cross section
of
CHMA
Projector
Reflected
light
Integrated
image
Transmitted
light
Real object
Transparent
material
Thin
concave mirror
array

Fig. 34.

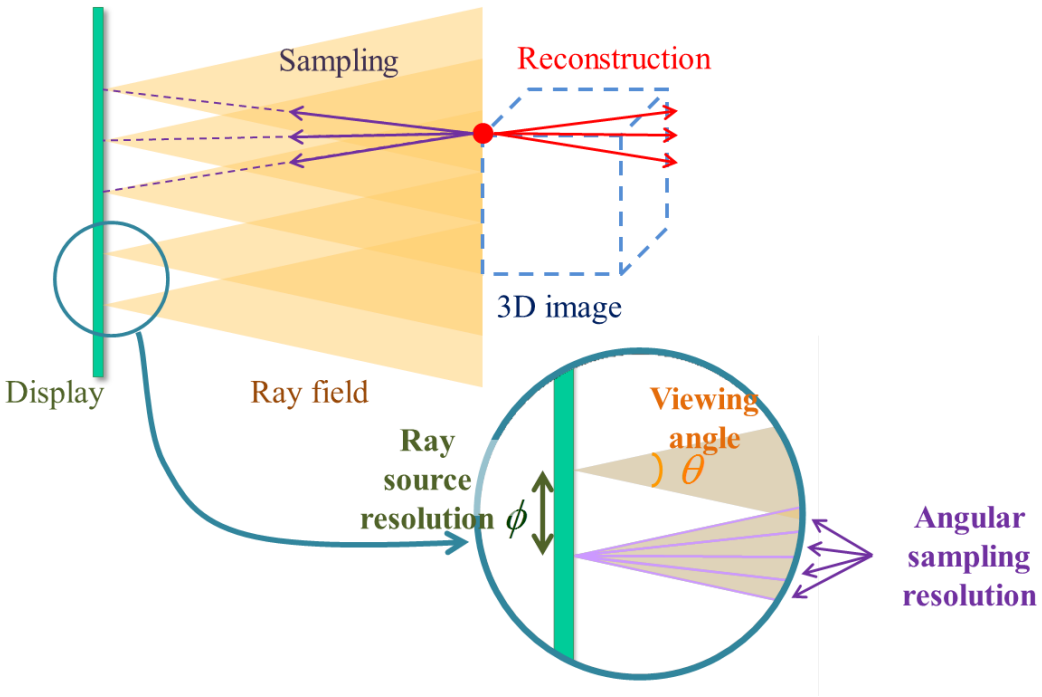
Sampling
Reconstruction
3D image
Display
Ray field
Viewing angle
θ
Ray source resolution
ϕ
Angular sampling resolution

(a)

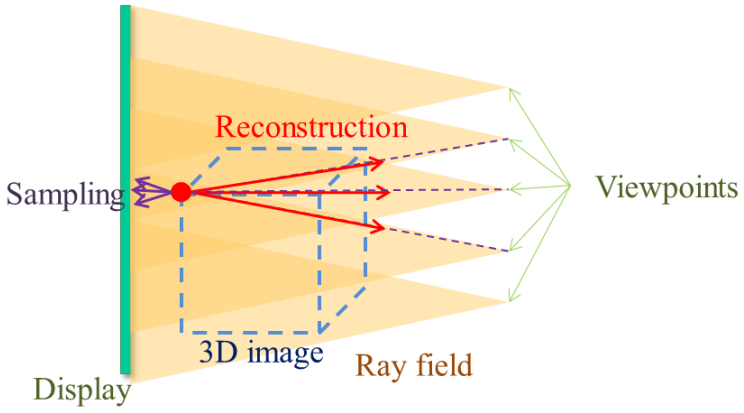
Reconstruction
Sampling
Viewpoints
3D image
Ray field
Display

(b)

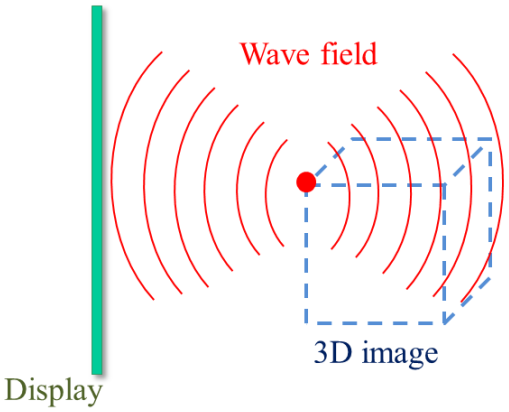
Wave field
3D image
Display

(c)

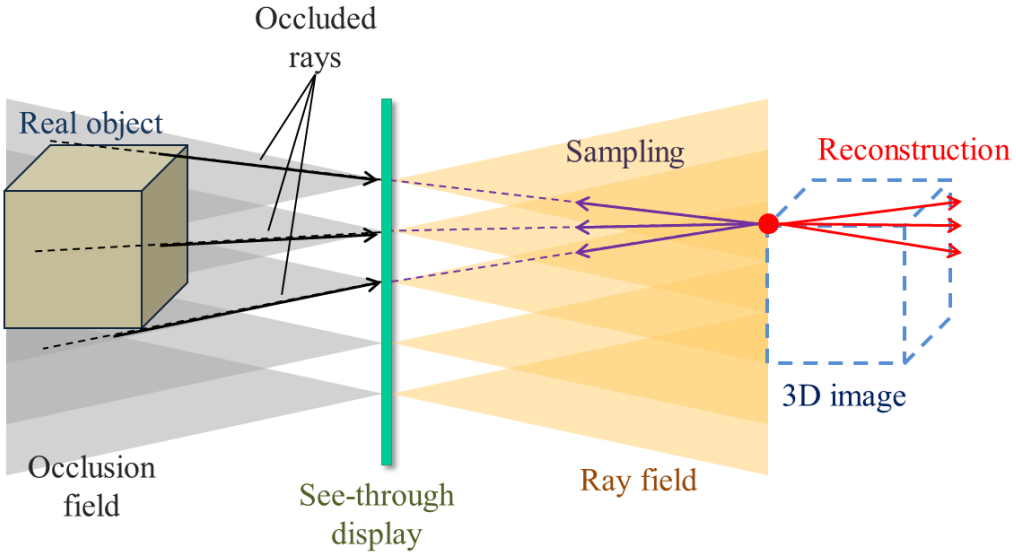
Occluded
rays
Real object
Sampling
Reconstruction
3D image
Occlusion
field
See-through
display
Ray field

(d)

Fig. 35.